

1 **Two Dimensional MXenes as Emerging Paradigm for Adsorptive Removal of**  
2 **Toxic Metallic Pollutants from wastewater**

3 Tahir Rasheed<sup>a\*</sup>, Fahmeeda Kausar<sup>b</sup>, Komal Rizwan<sup>c</sup> Muhammad Adeel<sup>d</sup>, Farooq Sher<sup>e</sup>, Sajjad  
4 Haider<sup>f</sup>

5 <sup>a</sup>Interdisciplinary Research Center for Advanced Materials, King Fahd University of Petroleum  
6 and Minerals (KFUPM), Dhahran 31261, Saudi Arabia.

7 <sup>b</sup>School of Chemistry and Chemical Engineering, Shanghai Jiao Tong University, Shanghai  
8 200240.

9 <sup>c</sup>Department of Chemistry University of Sahiwal, Sahiwal, 57000, Pakistan.

10 <sup>d</sup>Faculty of Applied Engineering, iPRACS, University of Antwerp, 2020 Antwerp, Belgium

11 <sup>e</sup>Department of Engineering, School of Science and Technology, Nottingham Trent University,  
12 Nottingham NG11 8NS, United Kingdom.

13 <sup>f</sup>Chemical Engineering Department, College of Engineering, King Saud University, P.O. Box 800,  
14 Riyadh 11421, Saudi Arabia.

15 \*Corresponding author emails: [masil@sjtu.edu.cn](mailto:masil@sjtu.edu.cn); [tahir.rasheed@hotmail.com](mailto:tahir.rasheed@hotmail.com) (T. Rasheed).

16 **Abstract**

17 Effective methods for removing harmful metals from wastewater have had a huge impact on  
18 reducing freshwater scarcity. Because of its excellent removal effectiveness, simplicity and low  
19 cost at ambient conditions, adsorption is one of the most promising purifying approaches. MXene-  
20 based nanoarchitectures have proven to be effective adsorbents in a variety of harmful metal  
21 removal applications. This owes from the distinctive features such as, hydrophilicity, high surface  
22 area, electron-richness, great adsorption capacity, and activated metallic hydroxide sites of  
23 MXenes. Given the rapid advancement in the design and synthesis of MXene nanoarchitectures for

24 water treatment, prompt updates on this research area are needed that focus on removal of toxic  
25 metal, such as production routes and characterization techniques for the advantages, merits and  
26 limitations of MXenes for toxic metal adsorption. This is in addition to the fundamentals and the  
27 adsorption mechanism tailored by the shape and composition of MXene based on some  
28 representative paradigms. Finally, the limits of MXenes are highlighted, as well as their potential  
29 future research directions for wastewater treatment. This manuscript may initiate researchers to  
30 improve unique MXene-based nanostructures with distinct compositions, shapes, and  
31 physiochemical merits for effective removal of toxic metals from wastewater.

32 **Keywords:** 2D-MXenes; MXene nanocomposite; wastewater; Adsorption; Toxic metal Pollutants

### 33 **1. Introduction**

34 As fast industrialization continues, various toxins have been released into water without being  
35 properly cleaned, causing serious environmental contamination and danger to human health  
36 (Jasper et al., 2017). Generally, Organic and inorganic pollutants are the two types of contaminants  
37 that can be found in the environment. Typical dye compounds such as methylene blue, which are  
38 released by manufacturers making paper, paint, textiles, and other products, are among the organic  
39 pollutants (Karaçetin et al., 2014). While heavy metal ions (HMIs) and radionuclide are among the  
40 inorganic pollutants in wastewater (Ahmad and Mirza, 2018; Mirza and Ahmad, 2018; Zhang et  
41 al., 2018). Because of their carcinogenicity and toxicity, they have adverse impact on natural  
42 environment and living organisms in general. Some of the maximum allowable contaminant level  
43 of heavy metals are as follows, Arsenic: .05 mg/l, Cadmium: .005 mg/l Lead: .015 mg/l, Mercury:  
44 .002 mg/l, Chromium: .1, Selenium: .05 mg/l, Antimony: .006 mg/l. Because some of them can  
45 bioaccumulate, the harm they cause to living organisms may be greater than that caused by  
46 pollutants that cannot bioaccumulate (Berrios et al., 2012; Karaçetin et al., 2014). As a result, one

47 of the most important predictors of long-term industrial prosperity has been the deployment of  
48 effective treatment procedures for the elimination of harmful toxins.

49 Adsorption is one of the most extensively employed technique for the purpose due to its appealing  
50 properties such as simplicity, cost-effectiveness, and applicability (Ahmad and Mirza, 2018;  
51 Burakov et al., 2018; Mirza and Ahmad, 2018; Wu et al., 2019; Mittal et al., 2021). Furthermore,  
52 using adsorbent to remove toxicants minimizes the production of secondary pollutants because the  
53 adsorbents absorb rather than reacting with the contaminants (Wu et al., 2019). A number of  
54 documented reports are present in the literature, which discuss the utility of powdered or granular  
55 activated carbon, chitosan, and kaolin etc. are the few among many to be used as adsorbents for  
56 the purpose (Oguz and Keskinler, 2005; Wang et al., 2010; Zhu et al., 2010). The greater surface  
57 area and high porosity of these materials makes them an ideal candidate for the environmental  
58 remediation. Recently, an emerging class of nanomaterials such as two-dimensional (2D) have  
59 extensively been exploited for the efficient removal of a variety of environmental contaminants.  
60 The distinctive features of these 2D nanomaterials warrant their applicability in adsorptive removal  
61 (Fu et al., 2018; Wu et al., 2019). The use of nanomaterial-based adsorbents for the treatment of  
62 organic and inorganic contaminants in water has increased due to the unique features of 2D  
63 nanomaterials, i.e. carbon-based nanomaterials (Atkovska et al., 2018). Nanomaterial-based  
64 adsorbents frequently have thin structures, large specific surface areas, and plentiful functional  
65 sites, as compared to the huge and bulkier construction of traditional adsorbents (Zhang et al.,  
66 2018). Because adsorbents must have a high level of contact with adsorbates and a sufficient  
67 surface area to function well, hence the nanomaterials are thought to have the ability to address  
68 both inorganic and organic adsorbates (Yang et al., 2019). MXene, a new class of 2D nanomaterials

69 derived from a family of transition metal nitride or carbide compounds, has recently piqued interest  
70 in a variety of fields.

71 Owing to their excellent properties such as greater surface area, eco-friendly, greater chemical  
72 stability, hydrophilicity, and electrical/thermal conductivity, MXenes are ideal materials for a  
73 variety of applications, such as hydrogen storage (Hu et al., 2013), lithium-ion battery (Naguib et  
74 al., 2012), supercapacitor (Zhu et al., 2016), semiconductor (Gao et al., 2016), and environmental  
75 applications (Ciou et al., 2019). Particularly, the probable environmental applications comprise of  
76 membrane filtration, photocatalysis and adsorption to eradicate contaminants, via MXenes and  
77 MXene-based composite materials as adsorbents for the elimination of inorganic and organic  
78 pollutants from water have extensively been studied (Rasool et al., 2017).

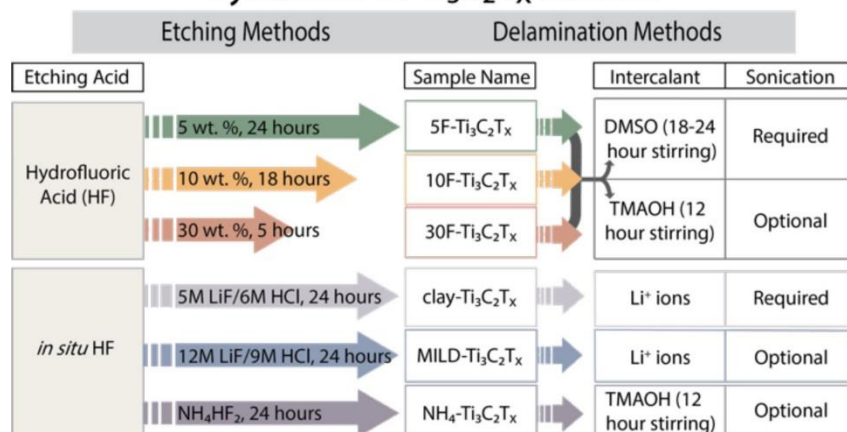
79 Herein, the main purpose of the study is to comprehend the overall knowledge of MXenes and  
80 their composites as potential adsorbent for the removal of inorganic impurities such as heavy metal  
81 ions and radionuclides from water. In order to achieve the goal, this study will focus on the key  
82 aspects of manipulating the composition and shape of MXenes and MXene based nanocomposites  
83 for the removal of toxic metal from wastewater, such as manufacturing strategies and  
84 characterization methodologies, as well as their formation mechanisms. The limitations and  
85 advantages of these materials as adsorbents of toxic heavy metals and radionuclides are reviewed,  
86 along with their adsorption mechanism, supported by several descriptive paradigms. Then,  
87 perspectives and outlooks for future research in the field of removing these analytes (heavy metal  
88 ions and radionuclides) are suggested.

## 89 **2. Characterization of MXenes and Their Preparation**

90 MXenes, a potentially new class of two dimensional (2D) materials, have been the subject of a  
91 number of recent book chapters and review papers that have discussed their distinctive features,  
92 potential applications, and syntheses (Ng et al., 2017; Zhang et al., 2018; Habib et al., 2019;  
93 Melchior et al., 2019). As a result, the focus of this review is solely on the adsorption behavior and  
94 characterization of certain MXene structures in wastewater treatment, with an emphasis on particle  
95 entrapment methods and the significance of unique surface functionalization in operational  
96 efficiency. The term “MXenes” represents a class of nanoparticles, sharing the general formula  
97 based representation as  $M_{n+1}X_nT_x$  ( $n = 1-3$ ). In this formula M stands for transition metals such  
98 as, Mo, Nb, Sc, Hf, Cr, Ti, Ta, Zr, V, etc. while X is a carbon or nitrogen atom and  $T_x$  is the  
99 variable surface termination which is highly dependent on the manufacturing method and  
100 requirement of properties of the formed MXene. These terminals may include fluorine, oxygen or  
101 hydroxyl moieties but not limited to them. The development in the field of MXenes as 2D materials  
102 using different methods and raw materials is becoming increasingly popular which is also  
103 emerging a new three dimensional (3D) constructs/architectures (Ng et al., 2017; Xiu et al., 2018).  
104 The layered architecture of M ( $n + 1$ ) and X ( $n$ ) layers respectively, which are termed 3D pores  
105 inside their nanoscale configuration, is what brands MXenes so intriguing (Anasori and Gogotsi,  
106 2019). While the majority of MXenes are made up of just one transition metal, some varieties exist  
107 in which more than one metal is involved, either in a layered fashion, random distribution or in  
108 well-ordered pattern. Generally, the selective etching by A group elements using their MAX phase  
109 is applied for the fabrication of MXenes. The layered nitrides and carbides (X-elements) represents  
110 the MAX phase in MXenes structure which are sandwich between A layers of group III A/IVA  
111 such as Si or Al (not limited to them may also include Pb, P, As, S, Ga, Sn, Ge, In, Cd, and Tl)  
112 and M layers of transition metals (Anasori and Gogotsi, 2019). Among the most commonly

113 commercially available MAX phase employed is  $Ti_3AlC_2$ . As a result, the majority of MXenes  
114 research focuses on those with the formula  $Ti_3C_2T_x$ , where T stands for surface terminations like  
115  $-OH$ ,  $F^-$ , or  $-O$ . The selective chemical etching methodology is being employed for the fabrication  
116 of  $Ti_3C_2T_x$ . The hydrofluoric acid (HF) is used as an etching agent, accompanied by the use of  
117 dimethyl sulfoxide as delaminating agent under sonication. Moreover, to create fluoride free  
118 surface termination the dry etching technique is widely exploited in comparison to wet etching.  
119 This can increase the suitability of activating the MXenes surface and its applicability in a broader  
120 context. The stacking of MXene layers and effects of various delamination and etching procedures  
121 on generated MXene formulae are portrayed in Figure 1 (Alhabeab et al., 2017). Herein, the  
122 influence of various preparatory methods of MXene and their structure, morphologies, and surface  
123 terminations are examined in relation to the hazardous metal. Before going into depth about  
124 MXenes' ability to remove harmful metal particles, it's important to note that one of the most  
125 significant roadblocks to MXenes' commercialization is its thermodynamically metastable  
126 condition. The remarkable high surface energy of MXenes, especially makes them highly  
127 susceptible to degradation. MXene solutions, in particular, oxidize over time, creating  $TiO_2$   
128 crystals at the boundaries of MXene flakes and eventually transforming the entire structure into  
129 carbon sheets and  $TiO_2$ . The difference between the oxidized and pristine MXene can be clearly  
130 marked by discerning the difference in color, as the oxidized solution colored as cloudy white or  
131 gray while the pristine MXenes are greenish black in color to the naked eye.

## Synthesis of $Ti_3C_2T_x$ MXene



132  
 133 **Figure 1.** Preparation of  $Ti_3C_2T_x$  using different synthesis routes (direct HF and in situ HF).  
 134 Reproduced with permission from (Alhabeab et al., 2017). Copyright 2017 ACS.

135 Generally, the MXenes powder are robust and stable in an oxygen rich atmosphere below 200 °C  
 136 (Zhang et al., 2017). For the remediation of toxicant such as metals,  $TiO_2$  is an effective adsorbent  
 137 for a variety of analytes including chromium (Almeida et al., 2019), mercury (Ghasemi et al.,  
 138 2012) and copper (Cheng et al., 2019). Consequently, a number of MXene based materials are  
 139 purposely venerable in hydrothermal environments to attain  $TiO_2$  as surface elements. Multiple  
 140 stabilizing strategies for MXene flakes have been investigated, including the use of carbon nano-  
 141 plates. This results in the creation of new MXene hybrids reinforced with  $MoS_2$  and carbon  
 142 accompanied by the high energy mechanical milling in DMSO demonstrating that the addition of  
 143 fluorine to their surfaces can achieve high stability (Wang et al., 2016; Wu et al., 2017).  
 144 Prospectively, MXene based compounds with greater shelf lives and higher stability are predicted  
 145 to be used in management of wastewater applications by taking fact that the MXene flakes are  
 146 exposed to aquatic environment. The fast degradability and fragility of MXenes should be  
 147 accountable when designing the systems for the remediation of targeted toxic metal. The profligate  
 148 conversion of MXenes into environment friendlier components is advantageous, which may

149 facilitate the operational simplicity in handling the resultant slurry to be used in wastewater  
150 management. Further investigations are needed to be carried out in defining their ranges of  
151 operation and final efficiency, more research into the applications of MXenes in water treatment,  
152 as well as their breakdown after binding with harmful metals or other harmful wastes, is required.

### 153 **3. Methods and factors effecting for the Removal of Toxic Metal from Wastewater**

154 Over the last few decades, various wastewater management systems have been developed  
155 (Burkhard et al., 2000). Among them, reverse osmosis, precipitation, adsorption ion exchange,  
156 membrane filtering, and electro-kinetic techniques are all traditional methodologies used for the  
157 removal of harmful metal (Vardhan et al., 2019). Even though some of these approaches, such as  
158 adsorption and ion exchange, are often employed concurrently, majority of them are used in  
159 tandem to isolate the harmful metal and other particles using isolation chambers or reverse  
160 osmosis. As a result, the poisonous metal solutes are subsequently converted to solid compounds  
161 using adsorption, precipitation, electro-kinetics, a chelating agent or coagulation, and subsequently  
162 filtered using different membranes or other collecting methods. Further, the preprocessing stages  
163 may involve the addition of some chemical agents or lime to achieve an ideal pH level, as well as  
164 temperature and fluid flow modifications, depending on the type of technique utilized. Moreover,  
165 post-operational processes can show a discrepancy but predominantly include dewatering, solid  
166 precipitates separation, transporting the solid waste to a landfill, as well as further treatment of the  
167 residual fluid till a suitable set of provisions is attained that sanctions it to be reverted to nature  
168 (Bhojwani et al., 2019; Ijanu et al., 2020). The formation of secondary pollutants in case of  
169 chemical precipitation, fouling and susceptibility by organic matter in the case of membranes, a  
170 limited ion removal margin, and a high energy cost in the case of electro-kinetic remediation are  
171 all obvious drawbacks in traditional wastewater treatment. Adsorption has showed promise among



172 all existing technologies due to its speedy operation and simplicity, specifically with the  
173 development of adsorbents that eliminate the requirement for secondary contaminant and  
174 processing. Eternally more and more inorganic and organic materials are being documented as  
175 potential adsorption mediators for the removal of toxic metal, such as activated carbon, rice husk,  
176 various bacterial species, palm fiber, chitosan, eggshells, clay, clinoptilolite, plants, and different  
177 types of nanomaterials (Nghah et al., 2011; Lim et al., 2018; Sherlala et al., 2018). Among them  
178 nanoparticles, whether inorganic or organic, have the most outstanding adsorption properties of all  
179 existing adsorbents, and some of them are already being used in the wastewater management  
180 business. In comparison to other adsorbents or chelating agents, the nanomaterials offer greater  
181 efficiency in handling the toxic metal pollutants. This high efficiency in remediating the metal  
182 based pollutants owes from the fact that the nanoparticles have high surface area and unique  
183 surface properties (Lim et al., 2018). Their surface characterization via different activation  
184 processes may enable harmful metal selectivity, allowing for future recycling of these particles  
185 rather than their disposal as toxic waste. The metal-organic frameworks (MOFs), Zeolites,  
186 bacterial exopolysaccharide, ceramics, algae, and carbons are examples of such type of  
187 nanomaterials. Activated carbon is the most extensively utilized nanomaterial in wastewater  
188 management, despite being a somewhat expensive choice (Skouteris et al., 2015; Dias and Petit,  
189 2016; Gupta and Diwan, 2017; Ahmadijokani et al., 2021). Future 2D nanostructures are rapidly  
190 improving in this ever-growing category because they have higher adsorption abilities due to their  
191 large functionalized surfaces with unique features that allow them to be integrated into a variety  
192 of wastewater treatment processes, either as adsorbents, catalytic and/or antibacterial agents, or  
193 functional membranes. The technique is still developing, and facing a number of issues in  
194 immediate commercialization of these materials. These drawbacks involve their short life span and

195 incompetent integration in the existing architecture of wastewater management systems (Rasool  
196 et al., 2019).

### 197 **3.1. Effect of pH**

198 The pH of the medium mainly effects the charge density and degree of ionization of the adsorbent  
199 and greatly affect the removal of metals. As at higher pH, hydroxide of metals are formed in the  
200 form of salts and become precipitate out from the system. This dependency mainly depends on  
201 element of adsorbent and chemistry of solution. The zeta potential measurements of MXene shows  
202 high charge density at pH lower than 2.41. In this way, the surface of the adsorbent can be  
203 negatively charged, positively charged or become neutral depending pH of the system.

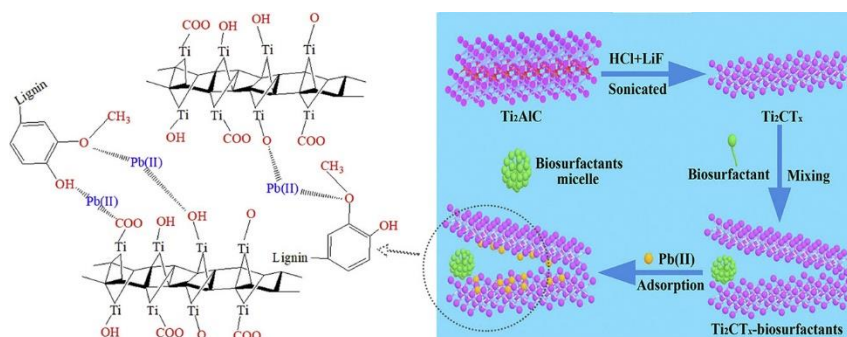
## 204 **4. MXene and MXene based composites for Toxic Metal Removal**

### 205 **4.1. Removal of Lead by MXene and MXene based composites**

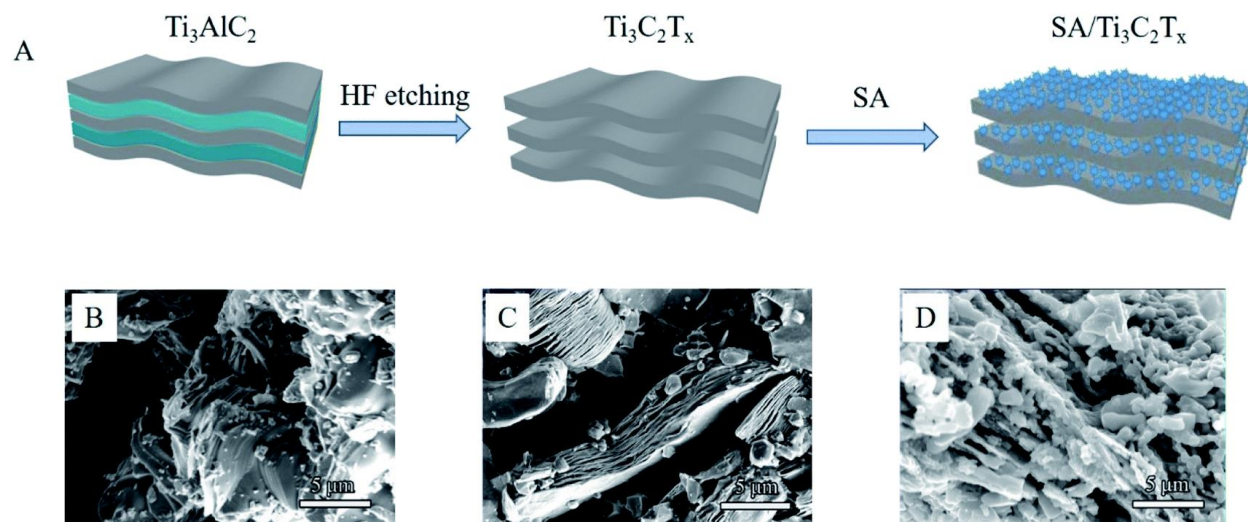
206 Lead is toxic metal that is produced from agricultural and industrial processes. High concentration  
207 of lead in aqueous matrices destroys the health of living beings. Peng and his colleagues used 2-D  
208 alkylated MXene ( $\text{Ti}_3\text{C}_2(\text{OH}/\text{ONa})_x\text{F}_{2-x}$ ) to adsorb Pb (II) from aqueous matrices in 5% sodium  
209 hydroxide solution for intercalation of sodium ions (Peng et al., 2014). Successful intercalation of  
210 sodium ions took place and they lead to expand the space among layers which enhanced the rate  
211 of diffusion of area which may react with Pb(II) ions. Significant adsorption of Pb (II) (140 mg/g)  
212 was observed and equilibrium was attained in 120s. The mechanism involved in this study was ion  
213 exchange. Presence of various elements like Ti, F, Na, O, and Pb was confirmed through elemental  
214 analysis and it was proposed that intercalated  $\text{H}^+$  and  $\text{Na}^+$  ions attached to Ti-O (negatively charged  
215 species) could exchange with Pb(II) (Giammar et al., 2007). Lead sorption on MXene flakes was  
216 found pH dependent and maximum adsorption was obtained in pH range of 5-7 ensuring ion

217 exchange as mechanism of action. At low pH values, MXenes showed less affinity towards Pb(II)  
218 ions which assist in regeneration of used MXene in acidic media. MXene material retained  
219 selectivity towards Pb (II) ions with efficacy of 95.2%. Jun and his colleagues used the MXene  
220 ( $\text{Ti}_3\text{C}_2\text{T}_x$ ) for removal of Pb(II) ions. MXene showed efficient adsorption and it was explained  
221 through pseudo-second-order kinetic and the Freundlich isotherm models and equilibrium was  
222 obtained in 30 min. MXene exhibited excellent reusability until four cycles (Jun et al., 2020a). Gu  
223 and his colleagues synthesized two different MXenes named e-TACFs and e-TACSs through  
224 hydrothermal method. e-TACFs and e-TACSs showed maximum adsorption of lead ions 284.9  
225 and 218.3 mg/g respectively. Ion exchange and complexation were found as mechanistic way of  
226 interaction of lead ions with MXenes which enhanced the adsorption potential. DFT studies  
227 supported the results (Gu et al., 2018b). The  $\text{Ti}_3\text{C}_2\text{T}_x$  powder contains great ion exchange potential  
228 but they show poor adsorption of heavy metals. Du and his colleagues overcome this drawback by  
229 regulating  $\text{Ti}_3\text{C}_2\text{T}_x$  powder with silane coupling agent (KH570) and they were found efficient for  
230 removal of lead ions. The modified powder possessed great surface area, thermal stability and  
231 good ion exchange potential. The  $\text{Ti}_3\text{C}_2\text{T}_x$  -KH570 powders showed adsorption potential of 147.29  
232 mg/g of Pb(II) ions while adsorption potential of pristine  $\text{Ti}_3\text{C}_2\text{T}_x$  powder was only 48.28 mg/g.  
233 hydroxyl groups of internal MXene were found responsible for adsorption of lead ions. The lead  
234 ions adsorption was dependent on availability of hydroxyl and carbonyl moieties of MXenes and  
235 KH570 respectively. Thus modified MXenes may be promising for removal of lead ions (Du et  
236 al., 2019). Similarly, in a latest study,  $\text{Ti}_2\text{CT}_x$  MXene sheets were functionalized with three  
237 different biosurfactants as chitosan, lignosulfonate and enzymatic hydrolysis lignin. The  
238 enzymatic hydrolysis lignin functionalized MXene showed high adsorption (232.9 mg/g) of Pb(II)  
239 ions and this may be attributed to prevention of  $\text{Ti}_2\text{CT}_x$  nanosheets from restacking and

240 incorporation of active functional moieties in MXene nanosheets due to enzymatic hydrolysis  
241 lignin biosurfactant (Figure 2) (Wang et al., 2020b). MXene has limited adsorption potential for  
242 metal ions and this may be because of limited adsorptive active sites. Dong and his colleagues  
243 synthesized MXene/alginate nanocomposite for adsorption of lead from aqueous solution (Figure  
244 3). This synthesized composite enhanced the adsorption potential and chelation capacity of Pb (II)  
245 ions. Maximum adsorption of Pb (II) was found to be 382.7 mg/g and equilibrium was reached  
246 within 15 mins. MXene/alginate composite can be regenerated with facile acid treatment without  
247 loss in activity. So this study showed that composites of MXenes may open new dimensions for  
248 high adsorptive removal of heavy metals with high efficacy at low temperature (Dong et al., 2019b)  
249 (Table 1).



251 **Figure 2:** Biosurfactant functionalized  $Ti_2CT_x$  MXene for adsorption of Pb(II) ions (Wang et al., 2020b)

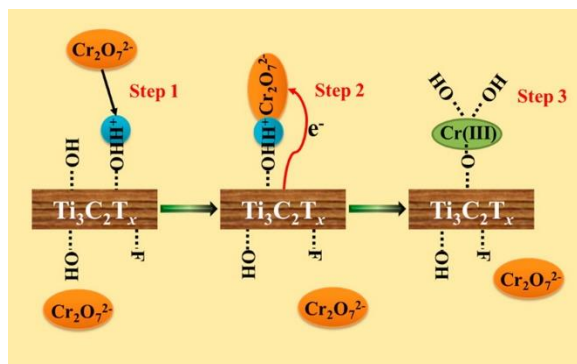


252  
 253 **Figure 3:** (A) Schematic of the preparation of the MXene/alginate composites; (B) surface morphology of  $Ti_3AlC_2$ ;  
 254 (C) surface morphology of  $Ti_3C_2T_x$ ; (D) surface morphology of the MXene/alginate composites (Dong et al., 2019b).  
 255 This article is licensed under a Creative Commons Attribution 3.0 Unported Licence.

#### 256 4.2. Reduction and Removal of Chromium Ions by MXene and MXene based composites

257 Chromium is toxic metal that is produced from different industries. Chromium may exist in  
 258 trivalent or hexavalent forms. Hexavalent chromium is carcinogenic. MXenes are known for  
 259 adsorption of high valent metal ions. Ying and his colleagues employed MXene nanosheets  
 260 ( $Ti_3C_2T_x$ ) for adsorption of Cr(VI) (Ying et al., 2015). MXene nanosheets efficiently adsorbed the  
 261 chromium metal ions with adsorption potential of 250 mg/g. Below pH 2, Cr(VI) were adsorbed  
 262 on positively charged nanosheets (due to presence of hydroxyl moieties) then hexavalent chromium  
 263 would reduce to trivalent chromium via electron transfer (Figure 4). Increase in pH would weaken  
 264 the electrostatic force of interactions, until pH reaches 13 and it stops completely. On contact with  
 265 MXene sheets the chromium metal is reduced with assistance of  $H^+$  ions and precipitates (pH 4.8)  
 266 and full precipitates are obtained at pH 5.6 where trivalent chromium may bind to MXene surface  
 267 in covalent manner via titanium oxide sites with 98% removal potential. Sheets may be degraded  
 268 after use. Urchin-like rutile MXene-based  $TiO_2-C/TiC$  nanocomposites were fabricated and they

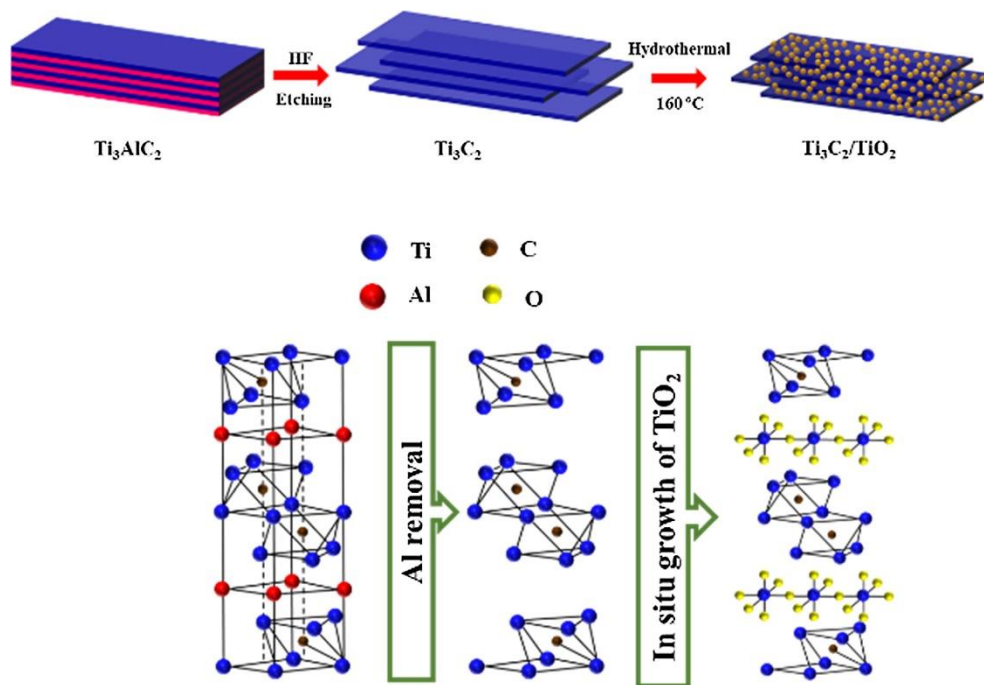
269 showed high adsorption of Cr (VI) with adsorption potential of 225 mg/g (Zou et al., 2016). MXene  
 270 flakes were used by group of scientists to adsorb chromium with adsorptive potential of 80 mg/g  
 271 at room temperature (Tang et al., 2018).



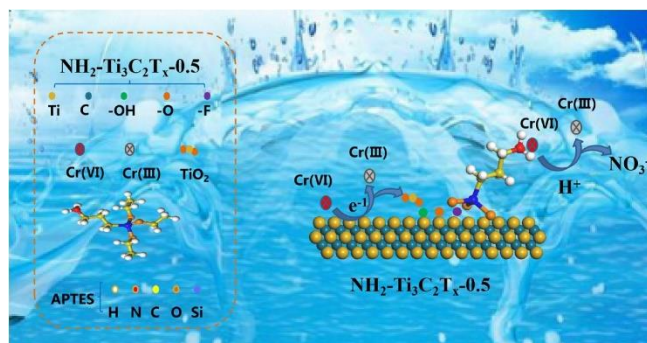
272  
 273 **Figure 4:** Illustration of the removal mechanism of (a) Cr(VI) by the Ti<sub>3</sub>C<sub>2</sub>T<sub>x</sub> nanosheets. Reprinted with  
 274 permission from Ref. (Ying et al., 2015)

275 The Ti<sub>3</sub>C<sub>2</sub>/TiO<sub>2</sub> composite attained effective removal of Cr(VI) from K<sub>2</sub>Cr<sub>2</sub>O<sub>7</sub> solution. The  
 276 mechanism involved is reduction of hexavalent chromium to trivalent chromium and then  
 277 adsorption of produced Cr (III) ions (Wang et al., 2020a). After synthesis of MXene flakes the  
 278 hydrogen fluoride was employed as etchant and obtained Ti<sub>3</sub>C<sub>2</sub> was heated hydrothermally to  
 279 grow Ti<sub>3</sub>C<sub>2</sub>/TiO<sub>2</sub> particles (Figure 5). The 24 h hydrothermal treatment gives optimum Cr (VI)  
 280 adsorption with reduction efficacy of 99.35%. Karthikeyan and his colleagues used 2D MXenes  
 281 for removal of Cr(VI). The removal rate of Cr (VI) was quick and reaction followed the second  
 282 order kinetics. Maximum adsorption capacity of Cr (VI) was found to be 104 mg/g. The MXene  
 283 sheets were regenerated by using 0.1 M sodium hydroxide solution. Adsorption phenomena  
 284 involved were electrostatic, complexation, surface interaction and ion exchange for uptake of Cr  
 285 (VI) ions (Karthikeyan et al., 2021) Recently amino functionalized MXenes (NH<sub>2</sub>-Ti<sub>3</sub>C<sub>2</sub>T<sub>x</sub>) were  
 286 synthesized. Amino moieties and Ti<sub>3</sub>C<sub>2</sub>T<sub>x</sub> sheets show synergistic effects in adsorption and  
 287 reduction of Cr (VI). The NH<sub>2</sub>-Ti<sub>3</sub>C<sub>2</sub>T<sub>x</sub> showed maximum adsorption potential of 107.4 mg/g for

288 Cr(VI) (Kong et al., 2021). Ti (II) and  $\text{NH}_3^+$  oxidized in Ti(IV) species and  $\text{NO}_3^-$  during the  
289 removal of Cr(VI). Amino functionalized MXene sheets showed great reusability and selectivity  
290 (Figure 6). Khan and his colleagues synthesized MXene and  $\delta\text{-MnO}_2/\text{MXene}$  hybrid through  
291 hydrothermal method for adsorption of Cr (VI). The pseudosecond-order model was  
292 followed. Adsorption of Cr (VI) was pH dependent. MXene and  $\delta\text{-MnO}_2/\text{MXene}$  hybrid showed  
293 maximum efficiently adsorbed the Cr (VI) with adsorption potential of 273.1 mg/g and  
294 353.87 mg/g respectively. The hybride of MXene with transition metal oxides showed highest  
295 adsorption potential and this may provide opportunity to remove heavy metals with efficiency due  
296 to electrostatic interactions (Khan et al., 2021). Composite of MXene with PEI modified sodium  
297 alginate aerogel was synthesized for removal of Cr (VI). MXene/PEI modified sodium  
298 alginate aerogel efficiently adsorbed the Cr (VI) with adsorption potential of 538.97 mg/g. The  
299 pseudo-second-order kinetic and Langmuir isotherm was followed. The composite strength was  
300 enhanced due to polymeric alginate and PEI. And composite showed efficiency uptill five cycles  
301 (Feng et al., 2021). Recently imidazole-MXene composite ( $\text{Ti}_3\text{C}_2@\text{IMIZ}$ ) were fabricated and it  
302 was used to remove Cr(VI) from medium. During adsorption, the Cr (VI) was converted to Cr (III)  
303 and removed through physical adsorption phenomena (electrostatic force of interaction). The  
304 composite was reproduce after use (Figure 7) (Yang et al., 2021) (Table 1). From reported work,  
305 it can be easily concluded that MXene composites are more suitable and efficient for removal of  
306 heavy metals in comparison of pristine MXenes.

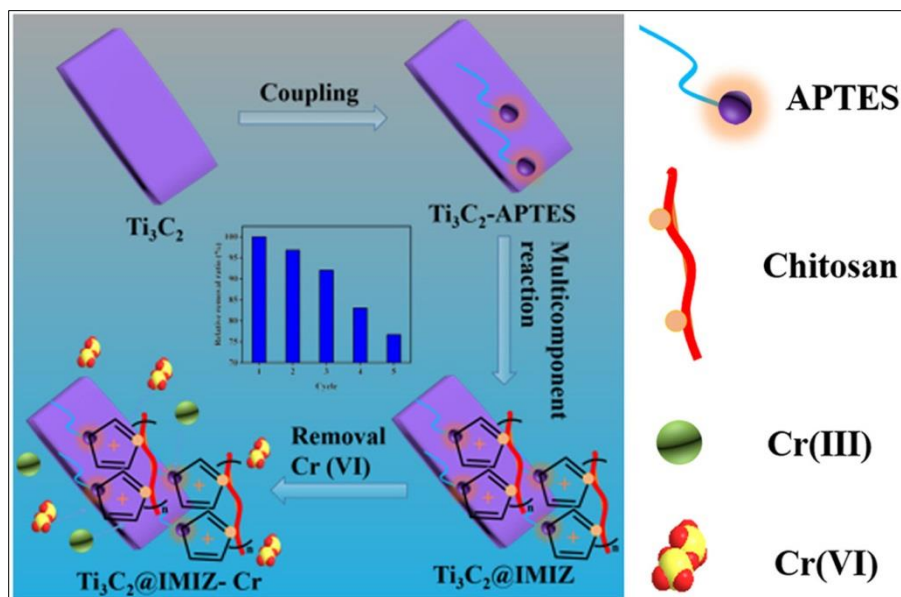


307  
 308 **Figure 5:** Schematic illustration of the preparation of  $\text{Ti}_3\text{C}_2/\text{TiO}_2$  composite. Adapted and reproduced with permission  
 309 (Wang et al., 2020a).



310  
 311 **Figure 6:** Amino-functionalized MXenes for efficient removal of Cr(VI) (Kong et al., 2021)  
 312





313

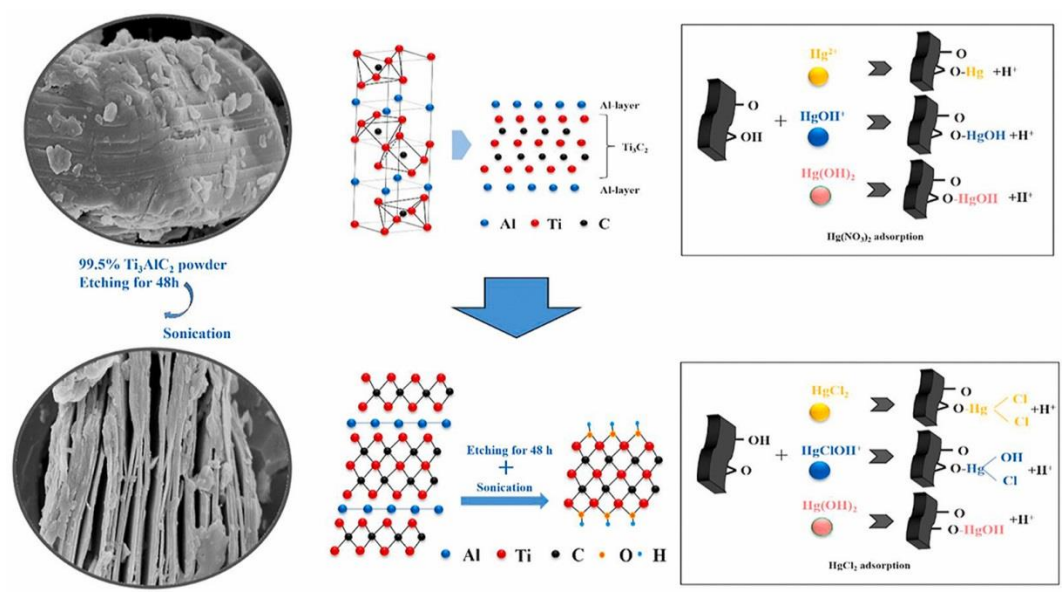
314 **Figure 7:** Synthesis and efficiency of Ti3C2@IMIZ for adsorptive removal of Cr(VI) (Yang et al., 2021)

### 315 **4.3. Removal of Mercury by MXene and MXene based composites**

316 Mercury pollution occurs due to burning of coal, waste materials. Various industries (cement,  
 317 paper and mining) are also responsible for mercury pollution. Mercury ions accumulate in human  
 318 body and cause severe health problems. Various studies have been conducted for removal of  
 319 mercury by using MXene base materials. In a study modified MXene flakes were used to adsorb  
 320 Hg (II) at different pH conditions. MXene flakes adsorbed the Hg (II) with adsorption potential of  
 321 1128.41 mg/g (Shahzad et al., 2018). MXene flakes were modified by magnetizing them to  
 322 enhance their stability and fast recovery. In another study compositing of MXene aerogel spheres  
 323 ( $Ti_3C_2T_x$ ) was carried out with varying concentrations of sodium alginate and this composite (MX-  
 324 SA) was used for removal of mercuric ions. High porosity, surface area and oxygenated  
 325 functionalities of MXene composite made it eligible to adsorb high amount of Hg(II). The MX-  
 326 SA<sub>4:20</sub> spheres showed exceptional adsorption potential of 932.84 mg/g for Hg(II) while MX-

327 SA<sub>2:20</sub> also adsorbed the Hg(II) (365 mg/g). This composite showed excellent results at various pH  
 328 conditions (Shahzad et al., 2019). Shahzad and his colleagues fabricated the molybdenum-  
 329 disulfide functionalized MXenes (MoS<sub>2</sub>/MX) for removal of Hg(II) ions. Synergistic effect of  
 330 sulfur and oxygenated MXene assisted to obtain highest adsorption of Hg ions with adsorption  
 331 potential of 1435.2 mg/g (Shahzad et al., 2020). This composite worked under both acidic and  
 332 basic media. This study exhibited that heterogenous composites can be used to remove heavy  
 333 metals. Fu and his colleagues employed multilayered Ti<sub>3</sub>C<sub>2</sub>O<sub>x</sub> MXene for removal of Hg (II) with  
 334 adsorption potential of 4806 mg/g (Fu et al., 2020). In another study, MXene was used to adsorb  
 335 Hg(II) from solutions containing mercuric nitrate and mercuric chloride. From mercuric nitrate  
 336 and mercuric chloride solution, 1057.3 mg/g 773.29 mg/g Hg(II) was adsorbed by MXene  
 337 material at temperature 30 °C (pH 5). Even at low pH values adsorption potential was maintained  
 338 (Figure 8) (Hu et al., 2021) (Table 1).

339



340

341 Figure 8: Efficiency of oxygen-containing MXene for removal of Hg(II) from solution of mercuric chloride and  
342 mercuric nitrate (Hu et al., 2021).

#### 343 **4.4. Removal of Copper Ions by MXene and MXene based composites**

344 MXene based materials have been used for removal of copper. Exfoliated MXene nanosheets were  
345 synthesized through ultrasonication under nitrogen atmosphere.  $Ti_3C_2T_x$  showed great efficacy for  
346 copper removal because of large surface area, porosity, hydrophilicity and novel structural  
347 features. The adsorption occurs at oxygenated functional moieties on surface of MXene which  
348 assists in reduction of Cu(II) ions and forming  $CuO_2$ ,  $CuO$  species. The delaminated MXene  
349 showed adsorption capacity around 78.45 mg/g of copper (Shahzad et al., 2017). Surface oxidation  
350 of MXenes take place after and before adsorption of copper ions. Adsorption of copper was found  
351 pH dependent. As low adsorption occurs at low pH values. After completion of adsorption, the  
352 MXene flakes showed no regeneration ability. Dong and his colleagues synthesized the hydrochar-  
353 wrapped MAX based nanofiber composites. The synthesized composites showed potential for  
354 removal of copper ions (Dong et al., 2019a). Recently rutile  $TiO_2@d-Ti_3C_2T_x$  hybrid has been  
355 used for adsorption of Cu (II) ions with maximum adsorption potential of 95 mg/g (Elumalai et  
356 al., 2020). Likewise MXenes ( $Ti_3C_2T_x$ ) functionalized with levodopa (DOPA) showed higher  
357 adsorption potential of Cu (II) ions with adsorption potential of 18.36 mg/g (Gan et al., 2020).  
358 Composite of MXene with sodium alginate also achieved high adsorption of Cu (II) ions with  
359 adsorption potential of 87.6 mg/g and equilibrium was reached in 15 minutes (Dong et al., 2019b).  
360 So MXene composites may be highly valuable for removal of heavy metals in comparison of virgin  
361 MXene (Table 1).

#### 362 **4.5. Removal/Extraction of Barium by MXene and MXene based composites**

363 Barium is a white shiny metal exist in environment in the form of different compound. It mainly  
 364 presents as barium oxide, barium sulfide, barium nitrite and barium halide. The oxidation of  
 365 barium produce hydrogen in water and become soluble in water species.

366 **Table 1: MXene and MXene based nanomaterials for removal of heavy metal ions**

Sr #	MXene	Targeted metal	Adsorption capacity	Mechanism	References
<b>Removal of Lead ions</b>					
1	e-TACSS e-TACFs	Pb(II)	218 mg/g, 284.9 mg/g	Adsorption	(Gu et al., 2018a)
2	Ti <sub>3</sub> C <sub>2</sub> (OH/ONa) <sub>x</sub> F <sub>2-x</sub>	Pb (II)	140 mg/g	Adsorption	(Peng et al., 2014)
3	Ti <sub>3</sub> C <sub>2</sub> T <sub>x</sub>	Pb(II)	36.6	Adsorption	(Jun et al., 2020a)
4	MXene/alginate nanocomposite	Pb(II)	382.7 mg/g	Adsorption	(Dong et al., 2019b)
5	Ti <sub>3</sub> C <sub>2</sub> T <sub>x</sub> -KH570	Pb(II)	147.29	Adsorption	(Du et al., 2019)
6	Enzymatic hydrolysis lignin functionalized Ti <sub>2</sub> CT <sub>x</sub> MXene	Pb(II)	232.9 mg/g	Adsorption	(Wang et al., 2020b).
7	MAX@titanate	Pb(II)	328.9 mg/g	Adsorption	(Gu et al., 2019)
8	AlkMXene-NH <sub>2</sub>	Pb(II)	384.63 mg/g	Adsorption	(Zhang et al., 2020)
<b>Removal of chromium ions</b>					
9	Ti <sub>3</sub> C <sub>2</sub> T <sub>x</sub> MXene nanosheets	Cr (VI)	104 mg/g	Adsorption	(Karthikeyan et al., 2021)
10	NH <sub>2</sub> -Ti <sub>3</sub> C <sub>2</sub> T <sub>x</sub>	Cr (VI)	107.4 mg/g	Adsorption	(Kong et al., 2021)
11	nZVI-Alk-Ti <sub>3</sub> C <sub>2</sub> composites	Cr (VI)	194.87 mg/g	Adsorption	(He et al., 2020)
12	MXene	Cr (VI)	273.1	Adsorption	(Khan et al., 2021)
13	δ-MnO <sub>2</sub> /MXene	Cr (VI)	353.87 mg/g	Adsorption	(Khan et al., 2021)

14	MXene/PEI modified sodium alginate aerogel	Cr (VI)	538.97 mg/g	Adsorption	(Feng et al., 2021)
15	MXenes/TiO <sub>2</sub>	Cr (VI)	49.67 mg/g	Adsorption	(Wang et al., 2020a)
16	Ti <sub>3</sub> C <sub>2</sub>	Cr (VI)	28.3 mg/g	Adsorption	(Tang et al., 2018)
17	Ti <sub>3</sub> C <sub>2</sub> T <sub>x</sub> -based films	Cr (VI)	84 mg/g	Adsorption	(Xie et al., 2019)
18	Ti <sub>3</sub> C <sub>2</sub> @IMIZ	Cr (VI)	119.5 mg/g	Adsorption	(Yang et al., 2021)
19	Fe <sub>3</sub> O <sub>4</sub> @MXene	Cr (VI)	70.2%	Adsorption	(Yang et al., 2020)
20	Ti <sub>3</sub> C <sub>2</sub> T <sub>x</sub> /PmPD-5/1	Cr (VI)	540.47 mg/g	Reduction/adsorption	(Jin et al., 2020)
<b>Removal of mercury ions</b>					
21	Magnetized MXene flakes	Hg (II)	1128.41 mg/g	Adsorption	(Shahzad et al., 2018)
22	MX-SA <sub>4:20</sub> MX-SA <sub>2:20</sub>	Hg(II)	932.84 mg/g 365 mg/g	Adsorption	(Shahzad et al., 2019)
23	MoS <sub>2</sub> /MX	Hg(II)	1435.2 mg/g	Adsorption	(Shahzad et al., 2020).
24	Ti <sub>3</sub> C <sub>2</sub> O <sub>x</sub> MXene	Hg(II)	4806 mg/g	Adsorption/reduction	(Fu et al., 2020)
25	MXene	Hg(II)	1057.3 mg/g from mercuric nitrate and 773.29 mg/g from mercuric chloride	Adsorption	(Hu et al., 2021)
<b>Removal of copper ions</b>					
26	Delaminated Ti <sub>3</sub> C <sub>2</sub> O <sub>x</sub> MXene	Cu (II)	78.45 mg/g	Adsorption	(Shahzad et al., 2017)
27	hydrochar-wrapped MAX based nanofibers	Cu (II)	-	Adsorption	(Dong et al., 2019a).
28	Amino acids modified MXenes (Ti <sub>3</sub> C <sub>2</sub> TX-PDOPA)	Cu (II)	18.36 mg/g	Adsorption	(Gan et al., 2020)
29	MXene/alginate composites	Cu (II)	87.6 mg/g	Adsorption	(Dong et al., 2019b)

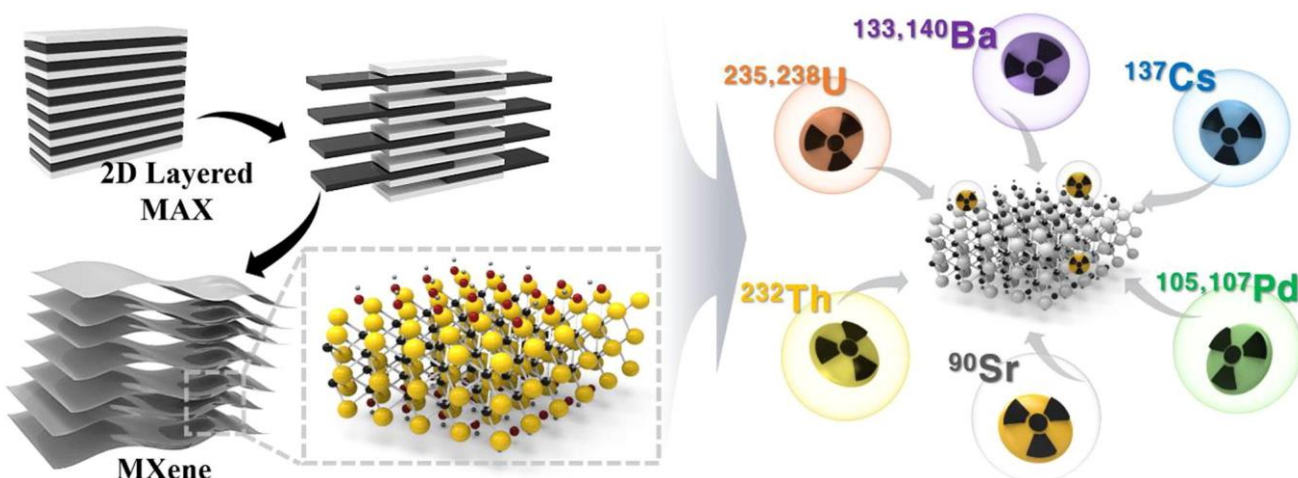
30	TiO <sub>2</sub> @ <i>d</i> - Ti <sub>3</sub> C <sub>2</sub> T <sub>x</sub> hybrid	Cu (II)	95 mg/g	Adsorption	(Elumalai et al., 2020)
----	---	---------	---------	------------	----------------------------

367

368 The compatibility with water make them spread on larger area and affect human and aquatic life  
369 (Ghaemi et al., 2011; Torab-Mostaedi et al., 2011). The limit of barium in water is set as 2 mg/L  
370 and 0.7 mg/L by USA EPA and WHO respectively (Edition, 2011). So, the presence of barium  
371 above this limit cause liver problem, increase in blood pressure, irritation in stomach, difficulty in  
372 breathing, heart rhythm change, swelling of brain, muscle weakness, kidney and heart damage and  
373 may act as a carcinogenic (Celebi et al., 2009). The main source of barium is oil and gas plants.  
374 To remove barium and its compounds, a number of method have been used include ion exchange,  
375 precipitation method, adsorption and membrane filtration (Fu and Wang, 2011; Kondash et al.,  
376 2014; Fard et al., 2016). Among them, adsorption is low cost, flexible and highly efficient method  
377 which is widely used to remove barium contaminants. A number of adsorbent have been  
378 established in this regard such as natural dolomite, chloriteillite, carbon based adsorbent, kaolinite  
379 and MXenes (Fu and Wang, 2011; Fard et al., 2016; Hadi et al., 2016). MXenes are highly efficient  
380 material with good capacity and economic benefits. In 2017 Fard and coworkers established  
381 MXene with HF solution and washed through dispersion by sonication in ethanol. The final  
382 product obtained by freeze-dried method of washed material for overnight. The MXene is  
383 synthesized by intercalation and exfoliation of titanium (III) carbide (II) (Ti<sub>3</sub>C<sub>2</sub>T<sub>x</sub>). In order to  
384 study the barium removal, they used this MXene as an adsorbent and with adsorption capacity 9.3  
385 mg/g with 100 % removal efficiency. The 90 % of barium was removed from the solution in first  
386 10 min selectively as compared to other metals present in solution. This adsorption of barium  
387 occurs through physisorption mechanism as a secondary route as shown in figure 9. In addition of  
388 this, Chemisorption work as a primary route by using functional groups terminated surface with –

389 O, –OH and –F. These functionalities form a chemical bonding with barium ion present in solution  
390 and generate barium hydroxide and barium fluoride (Fard et al., 2017). The applications of this  
391 MXene is limited in nuclear waste due to their less capacity of barium adsorption. To this end, Mu  
392 and his coworkers enhance the surface activity and metal intercalation of ( $\text{Ti}_3\text{C}_2\text{T}_x$ ) in order  
393 improve their adsorption capacity by the using NaOH (Mu et al., 2018). Through this treatment c-  
394 lattice parameter increased upto (2.09 nm) which improve the surface interaction affinities toward  
395 barium in solution. The functional groups anchoring at the surface shows excellent ability to absorb  
396 barium upto 46.46 mg/g. This absorption capacity is unpredictable and useful for nuclear waste  
397 management. The improvement of absorption capacity through NaOH is an efficient method. In  
398 2020 Jun et al. further improve the absorption ability of ( $\text{Ti}_3\text{C}_2\text{T}_x$ ) toward barium and strontium in  
399 waste water. They explain adsorption of barium via electrostatic attraction of negatively charged  
400 surface of ( $\text{Ti}_3\text{C}_2\text{T}_x$ ). They report an adsorption capacity upto 180 mg/g of barium in solution. The  
401 evidence the adsorption of barium through inner-sphere complexation, chemisorption and  
402 chemical ion exchange mechanism by FTIR, isothermal study, kinetic study and XPS respectively.  
403 The ( $\text{Ti}_3\text{C}_2\text{T}_x$ ) MXene adsorbent can be reused upto four cycles of adsorption and desorption (Jun  
404 et al., 2020b).

## 2D MXene Material for Removal of Radioactive Pollutants



405

406 Figure 9. Schematic illustration of 2D MXene based materials for the removal of radioactive  
407 pollutants from wastewater. Reproduced with permission from (Hwang et al., 2020). Copyright  
408 2020 Elsevier.

### 409 4.6. Removal of Palladium by MXene and MXene based composites

410 Palladium is a very versatile and useful materials in the field of electronics, catalysis, medicine,  
411 jewelry and dentistry with peculiar chemical and physical properties. The advancement in  
412 electronic device enhance the use and amount of palladium (Parodi et al., 2008; Won et al., 2014;  
413 Gupta and Diwan, 2017). The main source of palladium is from minerals, ores and waste  
414 electronic devices. It is also present in nuclear waste as Pd-107 and Pd-105 produce through the  
415 fission of uranium. This nuclear waste contains non-radioactive or less radioactive palladium (Can  
416 et al., 2013). To avoid its mixing with drinking water, Pd containing nuclear waste stored by  
417 vitrification and liquid containing Pd convert into glassy matrix. However, Pd presence in this  
418 nuclear waste can destroy vitrification and form a separate layer. In this sense, removal of Pd from  
419 nuclear waste is very important to avoid further contamination with drinking water (Abney et al.,



2014). A number of method has been employed in this direction include extraction, adsorption, precipitation and filtration (Khan et al., 2015; Mu et al., 2019). Among them, adsorption method seems to be efficient and easy due to its low cost, high efficiency and absence of organic solvents during applications. For this purpose, many adsorbents have been applied. Such as lignin, cellulose, carbon black and chitosan were used as inorganic adsorbent. They work with same principle to capture Pd from aqueous media (Kim et al., 2007; Sharma and Rajesh, 2014). Moreover, their low efficiency and high cost limited the applications. Therefore, it was required to design a new type of adsorbent with low cost and high efficiency. In this regard, transition metal carbide and carbontrides (MXene) are useful material produced by etching method. They pose good hydrophilic properties and readily available for water purification and pollutant adsorbent from environment. In 2019, Mu and his coworkers synthesized  $Ti_3C_2T_x$  based MXene by treating  $Ti_3AlC_2$  MAX with HF at different conditions. They synthesized this MXene for the removal of Pd from nitric acid media. The d-spacing of as synthesized MXene triggered at different temperature. As the temperature increase the d-spacing also increased. The d-spacing is directly related to adsorption ability of the material. So, MXene synthesized at 45 °C shows high adsorption power as compared to MXene synthesized at 25 °C and 35 °C. The adsorption efficiency is about 184.56 mg/g, which is higher as compare to other inorganic adsorbents due to higher surface area and d-spacing. The author concluded that the synthesis temperature has vital rule on the adsorption power of MXene (Mu et al., 2018).

#### 4.7. Removal of Cesium by MXene and MXene based composites

Cesium-137 is a radioactive isotopes produced during the fission process of uranium and other radioactive metals. The fission process is largely used in nuclear defense and for the production of nuclear energy. Moreover, nuclear destruction such as Fukushima and Chernobyl also produce a

443 large quantity of nuclear waste in environment (Lee et al., 2017; Calì et al., 2018). As produce Cs-  
444 137 is a strong beta and gamma emitter with half-life of 30.17 years and become a major problem  
445 in nuclear waste (Tan et al., 2018). It is most harmful material due to its high mobility and  
446 solubility with water. Due to its same hydration radius with potassium it can replace potassium  
447 from human's body and move in the same way pharmacokinetically as potassium. More  
448 interestingly, it enters human and animal body through food like water, meet, fishes and plants.  
449 This addition in living organism damage the cells and cause cancer (Khan et al., 2019). In order  
450 to prevent problem caused by cesium, a number of method has been used for its safe disposal and  
451 removal from waste water and nuclear waste. This involve electro dialysis, ion exchange, solvent  
452 extraction, chemical precipitation, coagulation and membrane processing. They are less effective  
453 and non-economical as a large amount of nuclear waste is produced with the passage of time. On  
454 the other hand, adsorption is a useful technique to remove radioactive waste efficiently (Yang et  
455 al., 2018). In this direction, newly developed 2D transition metal carbide and nitrides has been  
456 employed as adsorbent for nuclear waste (Lei et al., 2015). Khan and his coworkers study the use  
457 of  $Ti_3C_2T_x$  as a collector of  $Cs^+$  ion from contaminated water through ingestion test. They study  
458 the adsorption of cesium in this MXene through Langmuir and Freundlich isotherm. This  
459 adsorbent shows maximum adsorption capacity up to 25.4 mg/g as a coherent with Freundlich  
460 isotherm. This adsorption capacity obtained in one minute at room temperature. The heterogeneity  
461 of the surface with hydroxyl, fluorine and oxygen groups and multilayer adsorption phenomenon  
462 of adsorbent revealed in this work. The adsorption mechanism based on the attachment of Cs ion  
463 at the interlayer space and pores of adsorbent in the presence of other ion like ( $Na^+$ ,  $Li^+$ ,  $K^+$ ,  $Sr^{2+}$   
464 and  $Mg^{2+}$ ) (Khan et al., 2019). More recently, Jun and coworkers employed adsorption test by  
465 using  $Ti_3C_2T_x$  MXene for the removal of radioactive isotopes like Cs-137 from nuclear waste and

466 compared the result with activated carbon as an adsorbent. They noticed that the adsorption ability  
467 of MXene was about 148 mg/g for Cs<sup>+</sup> ion as compared to porous carbon shows 80 mg/g. Although  
468 porous carbon has 47 times higher surface area as compared to MXene still have less adsorption  
469 capacity. This higher adsorption ability of MXene is due to higher negatively charged surface,  
470 which shows that, electrostatic interaction plays vital role for the adsorption of Cs<sup>+</sup> ion. In addition  
471 of electrostatic force among adsorbent and Cs<sup>+</sup> ion, ion exchange mechanism also involved with  
472 presence of other cation like (K<sup>+</sup>, Na<sup>+</sup>, Ca<sup>2+</sup>, and Mg<sup>2+</sup>) and organic acid (Jun et al., 2020b).

#### 473 **4.8. Removal of Uranium (U<sup>6+</sup>) by MXene and MXene based composites**

474 Uranium is one of the main constituent of nuclear fuel and contaminated the environment with  
475 half-life  $4.47 \times 10^9$  years. It can mix with soil and water during nuclear waste management, mining  
476 and reprocessing of nuclear fuel (Yusan and Akyil, 2008; Stewart et al., 2010). There are two main  
477 component of uranium present as toxicant U<sup>4+</sup> and U<sup>6+</sup> ions. Among them U<sup>6+</sup> ion greatly affect  
478 the environment due to its high solubility in water and high mobility (Schnug and Lottermoser,  
479 2013; Pidchenko et al., 2017). To reduce U<sup>6+</sup> ion in aqueous media different type of sorbent has  
480 been used include nanoporous polymer, hydrothermal carbon, zeolites, metal oxides and  
481 hydroxides, metal phosphates, graphene oxide and its derivative, metal chalcogen, metal organic  
482 frameworks, clays and covalent organic framework (Yang et al., 2014; Bai et al., 2015; Lee et al.,  
483 2015; Li et al., 2015; Wang et al., 2018). Another way to reduce U<sup>6+</sup> from aqueous media is to  
484 convert it from highly soluble U<sup>6+</sup> to sparingly soluble U<sup>4+</sup> (O'Loughlin et al., 2003; Sun et al.,  
485 2014) through bacteria, iron sulfide, chemical reductants, zerovalent materials, magnetite and  
486 soluble iron material have been investigated. To remove this radioactive waste more efficiently,  
487 two dimensional metal carbides and carbontrides known as MXene having permeable reactive  
488 barrier, good stability, high removal tendency and good tolerance have been employed (Ghidiu et

489 al., 2014; Anasori et al., 2017). In contrast with others adsorbent MXenes have hydrophilic nature,  
490 charged surface, good ion exchange ability, good resistant towards acids and flexible swelling.  
491 These characteristics make them attractive candidates for management of environmental toxic  
492 materials. A number of reports have been published in the recent years about the removal of  $U^{6+}$   
493 ion by using titanium carbide, chromium carbide and vanadium carbide have been investigated  
494 extensively. These MXene are used as batch, theoretical and spectroscopic techniques (Wang et  
495 al., 2017; Deng et al., 2019; Fan et al., 2019; Wang et al., 2020b; Zhang and Liu, 2020). Among  
496 them titanium carbide shows maximum removal capacity about 470 mg/g due to surface  
497 complexation with good electrostatic attraction toward  $U^{6+}$  ion as compare to vanadium carbide  
498 MXene (174 mg/g). Similarly, strong ion exchange ability of titanium based MXene also  
499 responsible for uranium uptake. This titanium based MXene also used in the form composites with  
500 good reproduction of  $U^{6+}$  ion after conversion to  $U^{4+}$  ion. The amidoxime group present in MXene  
501 also responsible for uranium removal through coordination with uranyl group and established a  
502 bidentate chelating complexes. These all peculiar properties of titanium based MXenes make them  
503 excellent adsorbent for the removal of  $U^{6+}$  ion from nuclear waste. Zhang and his coworkers  
504 measured uranyl adsorption of hydroxyl functionalized titanium carbide about 595.3 mg/g through  
505 density functional theory. They proposed that uranyl ions attach with deprotonated oxygen rather  
506 than protonated oxygen at the surface of MXene in the form of hydroxy group (Zhang et al., 2016).  
507 They reported hydrogen bonding as a dominant factor in uranium ion adsorption. On the other  
508 hand, adsorption at vanadium carbide MXene is due to -OH, -O, -F groups. Similarly, Wang and  
509 his group reduce the radionuclide waste by converting highly soluble  $U^{6+}$  into partially soluble  
510  $U^{4+}$ . This removal based on sorption-reduction mechanism with uptake ability 470 mg/g (Wang et  
511 al., 2018). Deng et al. established a novel heterostructures  $Ti_3C_2/SrTiO_3$  based MXene through

512 oxidation of superficial layer of titanium carbide precursor (Deng et al., 2019). They used this  
513 MXene on the base of photocatalytic mechanism for the removal of uranium as its oxides.

#### 514 **5. Limitations of MXenes and MXene based composites Regarding Toxic Metal Removal**

515 Despite significant advancements in MXene production, there are a number of drawbacks to using  
516 MXenes for the remediation of harmful metals from wastewater, including lower biocompatibility  
517 and durability, inappropriate reusability as well as great affinity for aggregation (Ihsanullah, 2020).  
518 Furthermore, rational MXene synthesis with controllable and well-defined surface chemistry  
519 continue to be a major challenge. There are more than 30 kinds of reported MXenes based  
520 compounds, majority of them were predicted theoretically, thus more effort is needed to  
521 functionalize and synthesize different varieties of MXene that are well suited for the experimental  
522 treatment of wastewater. Likewise, the biocompatibility and cytotoxicity of MXenes should also  
523 be investigated prior to use as a wastewater treatment material. Noticeably, water purification  
524 research concentrated solely on  $Ti_3C_2T_x$  ( $T = OH, F, \text{ and } O$ ), with little attention paid to other  
525 MXenes. On the other hand,  $Ti_3C_2T_x$  MXene holds trifling interlayer arrangement and have a  
526 tendency to restack in aqueous environment, which restrict its extensive use in eradicating toxic  
527 metals with great hydrated ionic radii. The surface accessibility, reusability, and stability of other  
528 MXenes and  $Ti_3C_2T_x$  for remediation of lethal metals from wastewater can easily be upgraded  
529 considerably through recombination with carbon derived materials having unique physiochemical  
530 characters and greater surface area as well as abundant, cheaper, and stable polymers (Jlassi et al.,  
531 2020; Xu et al., 2020). Moreover, the extensive research is yet to be needed related to the use of  
532 MXene nano-architectures in eliminating hazardous contaminants and toxic metals from raw  
533 wastewater. Also, there must be a detailed comparison between MXenes and other adsorbents such  
534 as graphene, nanomaterials, metal-organic frameworks (MOFs), covalent organic frameworks

535 (COFs)and carbon nanotubes etc. to have a clear and broader idea about their roles as removal  
536 agents from wastewater.

## 537 **6. Conclusions and Future Prospects**

538 MXenes are among the most promising 2D layered nano-architectures currently being researched  
539 for the remediation of various hazardous environmental pollutants applications, particularly for  
540 the heavy metals. In conclusion, we have covered the essentials of MXenes, including their  
541 preparation, characteristics and their extensive characterization. Further, the current advancement  
542 in the area of environmental remediation for the removal of heavy metals along with their  
543 limitations and drawbacks has been discussed. MXenes have been found to have good  
544 metals/heavy metals removal capabilities, and their effectiveness appears to be superior to that of  
545 other traditionally used 2D materials and other pollutant adsorbents. Undoubtedly, MXenes have  
546 emerged as prospective materials for the removal of metals/heavy metals, there are still a number  
547 of impediments to overwhelmed and many questions to be answered before they can be used in  
548 the field.

549 1. The number of experimentally documented MXenes are limited as compared to the one which  
550 are reported through computations/simulations. Except,  $Ti_3C_2T_x$  which is extensively been used as  
551 a promising candidate for the environmental remediation of organic dyes, heavy metals and other  
552 pollutants of the emerging concern, there are a number of MXenes based nano-architectures which  
553 are expected to play an emerging role for the purpose. It's important to explore and experimentally  
554 synthesize variety of MXenes with adequate functionalization, required physiochemical  
555 characteristics, high water stability, and high absorbability for further advancement in  
556 environmental remediation. Further, the area of major concern to construct MXenes based  
557 materials for environmental remediation should be the structural features such as, Hierarchical and

558 non-layered carbides as well as the exposure of the active metal component. This will be a  
559 challenging task to accomplish. Beyond flat films, various morphologies of MXenes, such as  
560 nanocages and nanotubes should also be an area of worth investigations for environmental  
561 applications. Also, the surface functionalities play key role in elucidating the adsorption ability of  
562 MXenes. In comparison to real-time production, the majority of the theoretical models and  
563 modeling were done on the assumption that the MXenes have uniform functionalities at the  
564 terminals. To acquire full insights into the prediction of experimental circumstances, precursors  
565 used to create designed MXenes with desired functional groups, and target pollutants, finite  
566 element modeling theoretical simulations and classical MD are extremely essential.

567 2. The adsorption of metals/heavy metals with hydrated ionic radii bigger than the d-spacing  
568 between the MXene sheets is limited by the restacking and narrow interlayer spacing of pristine  
569 MXenes. To encapsulate the metals/heavy metals, having bigger hydrated radii, this interlayer  
570 spacing can easily be adjusted by the introduction of some cross-linker or intercalants. This can  
571 easily enhance the adsorption capacity of MXenes.

572 3. It's worth noting that the delamination conditions and surface functionalities are important  
573 factors in determining MXenes' adsorption capabilities. Normally, MXenes produced by synthetic  
574 methods are functionalized with several termination groups randomly. As a result, developing  
575 synthetic techniques and post-treatments is critical in order to establish a homogenous functional  
576 group, which is a challenging problem. More crucially, due to the strong reactivity of the surface  
577 metal atoms, it is believed that metals/heavy metals removal utilizing non-terminated MXenes  
578 including surface metal atoms will be successful, this should be experimentally examined for  
579 adsorption applications. As HF is used as an etching agent for the preparation of number of  
580 MXenes so, to develop a fluorine free strategy, which is another challenging factor to be addressed.

581 Till now, the most widely exploited methodology for the fabrication of MXenes is top-down  
582 method. This technique lacks in controlling the surface termination feature, which is most  
583 important parameter in finding the adsorption/removal ability of the synthesized material. This  
584 necessitates the development of bottom-up approach to synthesize the MXenes of desirable  
585 features

586 4. Given the rapid use and increasing quantity of MXene based materials, the acute toxicity of  
587 MXenes and their possible environmental risks should be thoroughly investigated. More study is  
588 needed to expand the spectrum of uses for environmentally benign MXenes in environmental  
589 remediation. To address the challenges and practical applicability concerning the environmental  
590 remediation, the competitive cost comparison between MXenes and other 2D adsorbents like  
591 graphene should be considered. Therefore, cheaper synthetic methodologies and MAX phase  
592 precursors should be taken into account. Hence, MXenes composed of naturally profuse elements  
593 are commended for accomplishing cost-effective environmental applications.

594 5. MXenes can easily be oxidized in the presence of water and degrade under different conditions.  
595 Therefore, the evaluation of different solvents towards their stability must be addressed with due  
596 care. The introduction of the MXenes to the polymeric matrices can be an option to increase the  
597 stability for future environmental applications. Furthermore, the desired functionalities can also be  
598 achieved by modifying the surface and manipulating the interlayer spacing via delamination and  
599 intercalation.

600 6. After adsorption it is really tedious to separate the MXenes from the solution, which limit them  
601 in-field practical utility for the separation of metals/heavy metals from the greater volume of  
602 solutions. MXenes can be incorporated into fibers or MXene derived composites having magnetic  
603 nano-architectures can be used to overcome this problem.



604 Conclusively, it is pertinent to say that this novel family of 2D materials has immense potential as  
605 adsorbents for the removal of metals/heavy metals. We believe that this study will provide a  
606 thorough overview of current research on the metals/heavy metals removal application of MXenes,  
607 as well as a significant push to further improve these systems for future environmental remediation  
608 research, particularly in the area of metals/heavy metals removal.

## 609 **Acknowledgment**

610 The authors sincerely appreciate funding from Researchers Supporting Project number (RSP-  
611 2021/399), King Saud University, Riyadh, Saudi Arabia

## 612 **Conflict of interest disclosure**

613 The representative authors have no conflict of interest to disclose in any capacity, either competing  
614 or financial.

## 615 **References**

- 616 Abney, C.W., Taylor-Pashow, K.M., Russell, S.R., Chen, Y., Samantaray, R., Lockard, J.V., Lin, W., 2014.  
617 Topotactic transformations of metal–organic frameworks to highly porous and stable inorganic sorbents  
618 for efficient radionuclide sequestration. *Chemistry of Materials* 26, 5231-5243.
- 619 Ahmad, R., Mirza, A., 2018. Facile one pot green synthesis of Chitosan-Iron oxide (CS-Fe<sub>2</sub>O<sub>3</sub>)  
620 nanocomposite: Removal of Pb(II) and Cd(II) from synthetic and industrial wastewater. *Journal of*  
621 *Cleaner Production* 186, 342-352.
- 622 Ahmadijokani, F., Tajahmadi, S., Bahi, A., Molavi, H., Rezakazemi, M., Ko, F., Aminabhavi, T.M., Arjmand,  
623 M., 2021. Ethylenediamine-functionalized Zr-based MOF for efficient removal of heavy metal ions from  
624 water. *Chemosphere* 264, 128466.
- 625 Alhabeb, M., Maleski, K., Anasori, B., Lelyukh, P., Clark, L., Sin, S., Gogotsi, Y., 2017. Guidelines for  
626 synthesis and processing of two-dimensional titanium carbide (Ti<sub>3</sub>C<sub>2</sub>T<sub>x</sub> MXene). *Chemistry of Materials*  
627 29, 7633-7644.
- 628 Almeida, J.C., Cardoso, C.E., Tavares, D.S., Freitas, R., Trindade, T., Vale, C., Pereira, E., 2019. Chromium  
629 removal from contaminated waters using nanomaterials—a review. *TrAC Trends in Analytical Chemistry*  
630 118, 277-291.
- 631 Anasori, B., Gogotsi, Y., 2019. Introduction to 2D transition metal carbides and nitrides (MXenes). *2D*  
632 *Metal carbides and nitrides (MXenes)*. Springer, pp. 3-12.
- 633 Anasori, B., Lukatskaya, M.R., Gogotsi, Y., 2017. 2D metal carbides and nitrides (MXenes) for energy  
634 storage. *Nature Reviews Materials* 2, 1-17.

635 Atkovska, K., Lisichkov, K., Ruseska, G., Dimitrov, A.T., Grozdanov, A., 2018. REMOVAL OF HEAVY METAL  
636 IONS FROM WASTEWATER USING CONVENTIONAL AND NANOSORBENTS: A REVIEW. Journal of  
637 Chemical Technology & Metallurgy 53.

638 Bai, Z.-Q., Yuan, L.-Y., Zhu, L., Liu, Z.-R., Chu, S.-Q., Zheng, L.-R., Zhang, J., Chai, Z.-F., Shi, W.-Q., 2015.  
639 Introduction of amino groups into acid-resistant MOFs for enhanced U (VI) sorption. Journal of Materials  
640 Chemistry A 3, 525-534.

641 Berrios, M., Martin, M.A., Martin, A., 2012. Treatment of pollutants in wastewater: Adsorption of  
642 methylene blue onto olive-based activated carbon. Journal of Industrial and Engineering Chemistry 18,  
643 780-784.

644 Bhojwani, S., Topolski, K., Mukherjee, R., Sengupta, D., El-Halwagi, M.M., 2019. Technology review and  
645 data analysis for cost assessment of water treatment systems. Science of the Total Environment 651,  
646 2749-2761.

647 Burakov, A.E., Galunin, E.V., Burakova, I.V., Kucherova, A.E., Agarwal, S., Tkachev, A.G., Gupta, V.K.,  
648 2018. Adsorption of heavy metals on conventional and nanostructured materials for wastewater  
649 treatment purposes: A review. Ecotoxicology and environmental safety 148, 702-712.

650 Burkhard, R., Deletic, A., Craig, A., 2000. Techniques for water and wastewater management: a review of  
651 techniques and their integration in planning. Urban water 2, 197-221.

652 Cali, E., Qi, J., Preedy, O., Chen, S., Boldrin, D., Branford, W., Vandeperre, L., Ryan, M., 2018.  
653 Functionalised magnetic nanoparticles for uranium adsorption with ultra-high capacity and selectivity.  
654 Journal of Materials Chemistry A 6, 3063-3073.

655 Can, M., Bulut, E., Örneke, A., Özacar, M., 2013. Synthesis and characterization of valonea tannin resin  
656 and its interaction with palladium (II), rhodium (III) chloro complexes. Chemical engineering journal 221,  
657 146-158.

658 Celebi, O., Kilikli, A., Erten, H., 2009. Sorption of radioactive cesium and barium ions onto solid humic  
659 acid. Journal of hazardous materials 168, 695-703.

660 Cheng, K., Cai, Z., Fu, J., Sun, X., Sun, W., Chen, L., Zhang, D., Liu, W., 2019. Synergistic adsorption of Cu  
661 (II) and photocatalytic degradation of phenanthrene by a jaboticaba-like TiO<sub>2</sub>/titanate nanotube  
662 composite: An experimental and theoretical study. Chemical Engineering Journal 358, 1155-1165.

663 Ciou, J.H., Li, S., Lee, P.S., 2019. Ti<sub>3</sub>C<sub>2</sub> MXene paper for the effective adsorption and controllable release  
664 of aroma molecules. Small 15, 1903281.

665 Deng, H., Li, Z.-j., Wang, L., Yuan, L.-y., Lan, J.-h., Chang, Z.-y., Chai, Z.-f., Shi, W.-q., 2019. Nanolayered  
666 Ti<sub>3</sub>C<sub>2</sub> and SrTiO<sub>3</sub> composites for photocatalytic reduction and removal of uranium (VI). ACS Applied  
667 Nano Materials 2, 2283-2294.

668 Dias, E.M., Petit, C., 2016. Correction: Towards the use of metal–organic frameworks for water reuse: a  
669 review of the recent advances in the field of organic pollutants removal and degradation and the next  
670 steps in the field. Journal of Materials Chemistry A 4, 3565-3565.

671 Dong, X., Wang, Y., Jia, M., Niu, Z., Cai, J., Yu, X., Ke, X., Yao, J., Zhang, X., 2019a. Sustainable and scalable  
672 in-situ synthesis of hydrochar-wrapped Ti<sub>3</sub>AlC<sub>2</sub>-derived nanofibers as adsorbents to remove heavy  
673 metals. Bioresource technology 282, 222-227.

674 Dong, Y., Sang, D., He, C., Sheng, X., Lei, L., 2019b. Mxene/alginate composites for lead and copper ion  
675 removal from aqueous solutions. RSC advances 9, 29015-29022.

676 Du, Y., Yu, B., Wei, L., Wang, Y., Zhang, X., Ye, S., 2019. Efficient removal of Pb(II) by Ti<sub>3</sub>C<sub>2</sub>T<sub>x</sub> powder  
677 modified with a silane coupling agent. Journal of Materials Science 54, 13283-13297.

678 Edition, F., 2011. Guidelines for drinking-water quality. WHO chronicle 38, 104-108.

679 Elumalai, S., Yoshimura, M., Ogawa, M., 2020. Simultaneous Delamination and Rutile Formation on the  
680 Surface of Ti<sub>3</sub>C<sub>2</sub>T<sub>x</sub> MXene for Copper Adsorption. Chemistry – An Asian Journal 15, 1044-1051.

681 Fan, M., Wang, L., Pei, C.-X., 2019. Alkalization intercalation of MXene for electrochemical detection of  
682 uranyl ion. JOURNAL OF INORGANIC MATERIALS-BEIJING- 34, 85-90.

683 Fard, A.K., Mckay, G., Chamoun, R., Rhadfi, T., Preud'Homme, H., Atieh, M.A., 2017. Barium removal  
684 from synthetic natural and produced water using MXene as two dimensional (2-D) nanosheet  
685 adsorbent. *Chemical engineering journal* 317, 331-342.

686 Fard, A.K., Rhadfi, T., Khraisheh, M., Atieh, M.A., Khraisheh, M., Hilal, N., 2016. Reducing flux decline and  
687 fouling of direct contact membrane distillation by utilizing thermal brine from MSF desalination plant.  
688 *Desalination* 379, 172-181.

689 Feng, Y., Wang, H., Xu, J., Du, X., Cheng, X., Du, Z., Wang, H., 2021. Fabrication of MXene/PEI  
690 functionalized sodium alginate aerogel and its excellent adsorption behavior for Cr(VI) and Congo Red  
691 from aqueous solution. *Journal of Hazardous Materials* 416, 125777.

692 Fu, F., Wang, Q., 2011. Removal of heavy metal ions from wastewaters: a review. *Journal of*  
693 *environmental management* 92, 407-418.

694 Fu, K., Liu, X., Yu, D., Luo, J., Wang, Z., Crittenden, J.C., 2020. Highly Efficient and Selective Hg(II) Removal  
695 from Water Using Multilayered Ti<sub>3</sub>C<sub>2</sub>O<sub>x</sub> MXene via Adsorption Coupled with Catalytic Reduction  
696 Mechanism. *Environmental Science & Technology* 54, 16212-16220.

697 Fu, L., Yan, Z., Zhao, Q., Yang, H., 2018. Novel 2D nanosheets with potential applications in heavy metal  
698 purification: A review. *Advanced Materials Interfaces* 5, 1801094.

699 Gan, D., Huang, Q., Dou, J., Huang, H., Chen, J., Liu, M., Wen, Y., Yang, Z., Zhang, X., Wei, Y., 2020.  
700 Bioinspired functionalization of MXenes (Ti<sub>3</sub>C<sub>2</sub>TX) with amino acids for efficient removal of heavy metal  
701 ions. *Applied Surface Science* 504, 144603.

702 Gao, G., Ding, G., Li, J., Yao, K., Wu, M., Qian, M., 2016. Monolayer MXenes: promising half-metals and  
703 spin gapless semiconductors. *Nanoscale* 8, 8986-8994.

704 Ghaemi, A., Torab-Mostaedi, M., Ghannadi-Maragheh, M., 2011. Characterizations of strontium (II) and  
705 barium (II) adsorption from aqueous solutions using dolomite powder. *Journal of Hazardous Materials*  
706 190, 916-921.

707 Ghasemi, Z., Seif, A., Ahmadi, T.S., Zargar, B., Rashidi, F., Rouzbahani, G.M., 2012. Thermodynamic and  
708 kinetic studies for the adsorption of Hg (II) by nano-TiO<sub>2</sub> from aqueous solution. *Advanced Powder*  
709 *Technology* 23, 148-156.

710 Ghidui, M., Lukatskaya, M.R., Zhao, M.-Q., Gogotsi, Y., Barsoum, M.W., 2014. Conductive two-  
711 dimensional titanium carbide 'clay' with high volumetric capacitance. *Nature* 516, 78-81.

712 Giammar, D.E., Maus, C.J., Xie, L., 2007. Effects of particle size and crystalline phase on lead adsorption  
713 to titanium dioxide nanoparticles. *Environmental Engineering Science* 24, 85-95.

714 Gu, P., Xing, J., Wen, T., Zhang, R., Wang, J., Zhao, G., Hayat, T., Ai, Y., Lin, Z., Wang, X., 2018a.  
715 Experimental and theoretical calculation investigation on efficient Pb (II) adsorption on etched Ti<sub>3</sub>AlC<sub>2</sub>  
716 nanofibers and nanosheets. *Environmental Science: Nano* 5, 946-955.

717 Gu, P., Xing, J., Wen, T., Zhang, R., Wang, J., Zhao, G., Hayat, T., Ai, Y., Lin, Z., Wang, X., 2018b.  
718 Experimental and theoretical calculation investigation on efficient Pb(ii) adsorption on etched Ti<sub>3</sub>AlC<sub>2</sub>  
719 nanofibers and nanosheets. *Environmental Science: Nano* 5, 946-955.

720 Gu, P., Zhang, S., Zhang, C., Wang, X., Khan, A., Wen, T., Hu, B., Alsaedi, A., Hayat, T., Wang, X., 2019.  
721 Two-dimensional MAX-derived titanate nanostructures for efficient removal of Pb(ii). *Dalton*  
722 *Transactions* 48, 2100-2107.

723 Gupta, P., Diwan, B., 2017. Bacterial exopolysaccharide mediated heavy metal removal: a review on  
724 biosynthesis, mechanism and remediation strategies. *Biotechnology Reports* 13, 58-71.

725 Habib, I., Ferrer, P., Ray, S.C., Ozoemena, K.I., 2019. Interrogating the impact of onion-like carbons on  
726 the supercapacitive properties of MXene (Ti<sub>2</sub>CTX). *Journal of Applied Physics* 126, 134301.

727 Hadi, P., Ning, C., Kubicki, J.D., Mueller, K., Fagan, J.W., Luo, Z., Weng, L., McKay, G., 2016. Sustainable  
728 development of a surface-functionalized mesoporous aluminosilicate with ultra-high ion exchange  
729 efficiency. *Inorganic Chemistry Frontiers* 3, 502-513.

730 He, L., Huang, D., He, Z., Yang, X., Yue, G., Zhu, J., Astruc, D., Zhao, P., 2020. Nanoscale zero-valent iron  
731 intercalated 2D titanium carbides for removal of Cr(VI) in aqueous solution and the mechanistic aspect.  
732 *Journal of Hazardous Materials* 388, 121761.

733 Hu, Q., Sun, D., Wu, Q., Wang, H., Wang, L., Liu, B., Zhou, A., He, J., 2013. MXene: a new family of  
734 promising hydrogen storage medium. *The Journal of Physical Chemistry A* 117, 14253-14260.

735 Hu, X., Chen, C., Zhang, D., Xue, Y., 2021. Kinetics, isotherm and chemical speciation analysis of Hg( II )  
736 adsorption over oxygen-containing MXene adsorbent. *Chemosphere* 278, 130206.

737 Hwang, S.K., Kang, S.-M., Rethinasabapathy, M., Roh, C., Huh, Y.S., 2020. MXene: An emerging two-  
738 dimensional layered material for removal of radioactive pollutants. *Chemical Engineering Journal* 397,  
739 125428.

740 Ihsanullah, I., 2020. MXenes (two-dimensional metal carbides) as emerging nanomaterials for water  
741 purification: Progress, challenges and prospects. *Chemical Engineering Journal* 388, 124340.

742 Ijanu, E., Kamaruddin, M., Norashiddin, F., 2020. Coffee processing wastewater treatment: a critical  
743 review on current treatment technologies with a proposed alternative. *Applied Water Science* 10, 1-11.

744 Jasper, J.T., Yang, Y., Hoffmann, M.R., 2017. Toxic byproduct formation during electrochemical  
745 treatment of latrine wastewater. *Environmental science & technology* 51, 7111-7119.

746 Jin, L., Chai, L., Yang, W., Wang, H., Zhang, L., 2020. Two-dimensional titanium carbides (Ti<sub>3</sub>C<sub>2</sub>T<sub>x</sub>)  
747 functionalized by poly (m-phenylenediamine) for efficient adsorption and reduction of hexavalent  
748 chromium. *International journal of environmental research and public health* 17, 167.

749 Jlassi, K., Eid, K., Sliem, M.H., Abdullah, A.M., Chehimi, M.M., Krupa, I., 2020. Rational synthesis,  
750 characterization, and application of environmentally friendly (polymer-carbon dot) hybrid composite  
751 film for fast and efficient UV-assisted Cd<sup>2+</sup> removal from water. *Environmental Sciences Europe* 32, 1-  
752 13.

753 Jun, B.-M., Her, N., Park, C.M., Yoon, Y., 2020a. Effective removal of Pb (ii) from synthetic wastewater  
754 using Ti<sub>3</sub>C<sub>2</sub>T<sub>x</sub> MXene. *Environmental Science: Water Research & Technology* 6, 173-180.

755 Jun, B.-M., Park, C.M., Heo, J., Yoon, Y., 2020b. Adsorption of Ba<sup>2+</sup> and Sr<sup>2+</sup> on Ti<sub>3</sub>C<sub>2</sub>T<sub>x</sub> MXene in model  
756 fracking wastewater. *Journal of environmental management* 256, 109940.

757 Karaçetin, G., Sivrikaya, S., Imamoğlu, M., 2014. Adsorption of methylene blue from aqueous solutions  
758 by activated carbon prepared from hazelnut husk using zinc chloride. *Journal of Analytical and Applied*  
759 *Pyrolysis* 110, 270-276.

760 Karthikeyan, P., Ramkumar, K., Pandi, K., Fayyaz, A., Meenakshi, S., Park, C.M., 2021. Effective removal  
761 of Cr(VI) and methyl orange from the aqueous environment using two-dimensional (2D) Ti<sub>3</sub>C<sub>2</sub>T<sub>x</sub> MXene  
762 nanosheets. *Ceramics International* 47, 3692-3698.

763 Khan, A.R., Awan, S.K., Husnain, S.M., Abbas, N., Anjum, D.H., Abbas, N., Benaissa, M., Mirza, C.R.,  
764 Mujtaba-ul-Hassan, S., Shahzad, F., 2021. 3D flower like δ-MnO<sub>2</sub>/MXene Nano-hybrids for the removal  
765 of hexavalent Cr from wastewater. *Ceramics International*.

766 Khan, A.R., Husnain, S.M., Shahzad, F., Mujtaba-ul-Hassan, S., Mehmood, M., Ahmad, J., Mehran, M.T.,  
767 Rahman, S., 2019. Two-dimensional transition metal carbide (Ti<sub>3</sub>C<sub>2</sub>T<sub>x</sub>) as an efficient adsorbent to  
768 remove cesium (Cs<sup>+</sup>). *Dalton Transactions* 48, 11803-11812.

769 Khan, T.A., Chaudhry, S.A., Ali, I., 2015. Equilibrium uptake, isotherm and kinetic studies of Cd (II)  
770 adsorption onto iron oxide activated red mud from aqueous solution. *Journal of Molecular Liquids* 202,  
771 165-175.

772 Kim, Y.-H., Ogata, T., Nakano, Y., 2007. Kinetic analysis of palladium (II) adsorption process on  
773 condensed-tannin gel based on redox reaction models. *Water research* 41, 3043-3050.

774 Kondash, A.J., Warner, N.R., Lahav, O., Vengosh, A., 2014. Radium and barium removal through blending  
775 hydraulic fracturing fluids with acid mine drainage. *Environmental science & technology* 48, 1334-1342.

776 Kong, A., Sun, Y., Peng, M., Gu, H., Fu, Y., Zhang, J., Li, W., 2021. Amino-functionalized MXenes for  
777 efficient removal of Cr(VI). *Colloids and Surfaces A: Physicochemical and Engineering Aspects* 617,  
778 126388.

779 Lee, H.Y., Kim, H.S., Jeong, H.-K., Park, M., Chung, D.-Y., Lee, K.-Y., Lee, E.-H., Lim, W.T., 2017. Selective  
780 removal of radioactive cesium from nuclear waste by zeolites: on the origin of cesium selectivity  
781 revealed by systematic crystallographic studies. *The Journal of Physical Chemistry C* 121, 10594-10608.

782 Lee, S.S., Li, W., Kim, C., Cho, M., Lafferty, B.J., Fortner, J.D., 2015. Surface functionalized manganese  
783 ferrite nanocrystals for enhanced uranium sorption and separation in water. *Journal of Materials*  
784 *Chemistry A* 3, 21930-21939.

785 Lei, J.-C., Zhang, X., Zhou, Z., 2015. Recent advances in MXene: Preparation, properties, and applications.  
786 *Frontiers of Physics* 10, 276-286.

787 Li, J., Yang, X., Bai, C., Tian, Y., Li, B., Zhang, S., Yang, X., Ding, S., Xia, C., Tan, X., 2015. A novel  
788 benzimidazole-functionalized 2-D COF material: Synthesis and application as a selective solid-phase  
789 extractant for separation of uranium. *Journal of colloid and interface science* 437, 211-218.

790 Lim, J.Y., Mubarak, N., Abdullah, E., Nizamuddin, S., Khalid, M., 2018. Recent trends in the synthesis of  
791 graphene and graphene oxide based nanomaterials for removal of heavy metals—A review. *Journal of*  
792 *Industrial and Engineering Chemistry* 66, 29-44.

793 Melchior, S.A., Palaniandy, N., Sigalas, I., Iyuke, S.E., Ozoemena, K.I., 2019. Probing the  
794 electrochemistry of MXene (Ti<sub>2</sub>CTx)/electrolytic manganese dioxide (EMD) composites as anode  
795 materials for lithium-ion batteries. *Electrochimica Acta* 297, 961-973.

796 Mirza, A., Ahmad, R., 2018. Novel recyclable (Xanthan gum/montmorillonite) bionanocomposite for the  
797 removal of Pb (II) from synthetic and industrial wastewater. *Environmental Technology & Innovation* 11,  
798 241-252.

799 Mittal, J., Ahmad, R., Mariyam, A., Gupta, V., Mittal, A., 2021. Expedient and enhanced sequestration  
800 of heavy metal ions from aqueous environment by papaya peel carbon: a green and low-cost adsorbent.  
801 *DESALINATION AND WATER TREATMENT* 210, 365-376.

802 Mu, W., Du, S., Li, X., Yu, Q., Wei, H., Yang, Y., Peng, S., 2019. Removal of radioactive palladium based on  
803 novel 2D titanium carbides. *Chemical Engineering Journal* 358, 283-290.

804 Mu, W., Du, S., Yu, Q., Li, X., Wei, H., Yang, Y., 2018. Improving barium ion adsorption on two-  
805 dimensional titanium carbide by surface modification. *Dalton Transactions* 47, 8375-8381.

806 Naguib, M., Come, J., Dyatkin, B., Presser, V., Taberna, P.-L., Simon, P., Barsoum, M.W., Gogotsi, Y.,  
807 2012. MXene: a promising transition metal carbide anode for lithium-ion batteries. *Electrochemistry*  
808 *Communications* 16, 61-64.

809 Ng, V.M.H., Huang, H., Zhou, K., Lee, P.S., Que, W., Xu, J.Z., Kong, L.B., 2017. Recent progress in layered  
810 transition metal carbides and/or nitrides (MXenes) and their composites: synthesis and applications.  
811 *Journal of Materials Chemistry A* 5, 3039-3068.

812 Ngah, W.W., Teong, L., Hanafiah, M.M., 2011. Adsorption of dyes and heavy metal ions by chitosan  
813 composites: A review. *Carbohydrate polymers* 83, 1446-1456.

814 O'Loughlin, E.J., Kelly, S.D., Cook, R.E., Csencsits, R., Kemner, K.M., 2003. Reduction of uranium (VI) by  
815 mixed iron (II)/iron (III) hydroxide (green rust): formation of UO<sub>2</sub> nanoparticles. *Environmental science &*  
816 *technology* 37, 721-727.

817 Oguz, E., Keskinler, B., 2005. Determination of adsorption capacity and thermodynamic parameters of  
818 the PAC used for bomaplex red CR-L dye removal. *Colloids and Surfaces A: Physicochemical and*  
819 *Engineering Aspects* 268, 124-130.

820 Parodi, A., Vincent, T., Pilsniak, M., Trochimczuk, A.W., Guibal, E., 2008. Palladium and platinum binding  
821 on an imidazol containing resin. *Hydrometallurgy* 92, 1-10.

822 Peng, Q., Guo, J., Zhang, Q., Xiang, J., Liu, B., Zhou, A., Liu, R., Tian, Y., 2014. Unique lead adsorption  
823 behavior of activated hydroxyl group in two-dimensional titanium carbide. *Journal of the American*  
824 *Chemical Society* 136, 4113-4116.

825 Pidchenko, I., Kvashnina, K.O., Yokosawa, T., Finck, N., Bahl, S., Schild, D., Polly, R., Bohnert, E., Rossberg,  
826 A., Göttlicher, J.r., 2017. Uranium redox transformations after U (VI) coprecipitation with magnetite  
827 nanoparticles. *Environmental science & technology* 51, 2217-2225.

828 Rasool, K., Mahmoud, K.A., Johnson, D.J., Helal, M., Berdiyrov, G.R., Gogotsi, Y., 2017. Efficient  
829 antibacterial membrane based on two-dimensional Ti<sub>3</sub>C<sub>2</sub>T<sub>x</sub> (MXene) nanosheets. *Scientific reports* 7,  
830 1-11.

831 Rasool, K., Pandey, R.P., Rasheed, P.A., Buczek, S., Gogotsi, Y., Mahmoud, K.A., 2019. Water treatment  
832 and environmental remediation applications of two-dimensional metal carbides (MXenes). *Materials*  
833 *Today* 30, 80-102.

834 Schnug, E., Lottermoser, B.G., 2013. Fertilizer-derived uranium and its threat to human health. ACS  
835 Publications.

836 Shahzad, A., Jang, J., Lim, S.-R., Lee, D.S., 2020. Unique selectivity and rapid uptake of molybdenum-  
837 disulfide-functionalized MXene nanocomposite for mercury adsorption. *Environmental Research* 182,  
838 109005.

839 Shahzad, A., Nawaz, M., Moztahida, M., Jang, J., Tahir, K., Kim, J., Lim, Y., Vassiliadis, V.S., Woo, S.H., Lee,  
840 D.S., 2019. Ti<sub>3</sub>C<sub>2</sub>T<sub>x</sub> MXene core-shell spheres for ultrahigh removal of mercuric ions. *Chemical*  
841 *Engineering Journal* 368, 400-408.

842 Shahzad, A., Rasool, K., Miran, W., Nawaz, M., Jang, J., Mahmoud, K.A., Lee, D.S., 2017. Two-Dimensional  
843 Ti<sub>3</sub>C<sub>2</sub>T<sub>x</sub> MXene Nanosheets for Efficient Copper Removal from Water. *ACS Sustainable Chemistry &*  
844 *Engineering* 5, 11481-11488.

845 Shahzad, A., Rasool, K., Miran, W., Nawaz, M., Jang, J., Mahmoud, K.A., Lee, D.S., 2018. Mercuric ion  
846 capturing by recoverable titanium carbide magnetic nanocomposite. *Journal of hazardous materials* 344,  
847 811-818.

848 Sharma, S., Rajesh, N., 2014. 2-Mercaptobenzothiazole impregnated cellulose prepared by  
849 ultrasonication for the effective adsorption of precious metal palladium. *Chemical Engineering Journal*  
850 241, 112-121.

851 Sherlala, A., Raman, A., Bello, M., Asghar, A., 2018. A review of the applications of organo-functionalized  
852 magnetic graphene oxide nanocomposites for heavy metal adsorption. *Chemosphere* 193, 1004-1017.

853 Skouteris, G., Saroj, D., Melidis, P., Hai, F.I., Ouki, S., 2015. The effect of activated carbon addition on  
854 membrane bioreactor processes for wastewater treatment and reclamation—a critical review.  
855 *Bioresource technology* 185, 399-410.

856 Stewart, B.D., Mayes, M.A., Fendorf, S., 2010. Impact of uranyl– calcium– carbonato complexes on  
857 uranium (VI) adsorption to synthetic and natural sediments. *Environmental science & technology* 44,  
858 928-934.

859 Sun, Y., Ding, C., Cheng, W., Wang, X., 2014. Simultaneous adsorption and reduction of U (VI) on reduced  
860 graphene oxide-supported nanoscale zerovalent iron. *Journal of Hazardous Materials* 280, 399-408.

861 Tan, X., Fang, M., Tan, L., Liu, H., Ye, X., Hayat, T., Wang, X., 2018. Core–shell hierarchical C@ Na<sub>2</sub>Ti<sub>3</sub>O<sub>7</sub>·9H<sub>2</sub>O  
862 nanostructures for the efficient removal of radionuclides. *Environmental Science: Nano* 5,  
863 1140-1149.

864 Tang, Y., Yang, C., Que, W., 2018. A novel two-dimensional accordion-like titanium carbide (MXene) for  
865 adsorption of Cr (VI) from aqueous solution. *Journal of Advanced Dielectrics* 8, 1850035.

866 Torab-Mostaedi, M., Ghaemi, A., Ghassabzadeh, H., Ghannadi-Maragheh, M., 2011. Removal of  
867 strontium and barium from aqueous solutions by adsorption onto expanded Perlite. *The Canadian*  
868 *journal of chemical engineering* 89, 1247-1254.

869 Vardhan, K.H., Kumar, P.S., Panda, R.C., 2019. A review on heavy metal pollution, toxicity and remedial  
870 measures: Current trends and future perspectives. *Journal of Molecular Liquids* 290, 111197.

871 Wang, G., Wang, X., Chai, X., Liu, J., Deng, N., 2010. Adsorption of uranium (VI) from aqueous solution on  
872 calcined and acid-activated kaolin. *Applied Clay Science* 47, 448-451.

873 Wang, H., Cui, H., Song, X., Xu, R., Wei, N., Tian, J., Niu, H., 2020a. Facile synthesis of heterojunction of  
874 MXenes/TiO<sub>2</sub> nanoparticles towards enhanced hexavalent chromium removal. *Journal of colloid and  
875 interface science* 561, 46-57.

876 Wang, K., Zhou, Y., Xu, W., Huang, D., Wang, Z., Hong, M., 2016. Fabrication and thermal stability of two-  
877 dimensional carbide Ti<sub>3</sub>C<sub>2</sub> nanosheets. *Ceramics International* 42, 8419-8424.

878 Wang, L., Song, H., Yuan, L., Li, Z., Zhang, Y., Gibson, J.K., Zheng, L., Chai, Z., Shi, W., 2018. Efficient U (VI)  
879 reduction and sequestration by Ti<sub>2</sub>CT x MXene. *Environmental science & technology* 52, 10748-10756.

880 Wang, L., Tao, W., Yuan, L., Liu, Z., Huang, Q., Chai, Z., Gibson, J.K., Shi, W., 2017. Rational control of the  
881 interlayer space inside two-dimensional titanium carbides for highly efficient uranium removal and  
882 imprisonment. *Chemical Communications* 53, 12084-12087.

883 Wang, S., Liu, Y., Lü, Q.-F., Zhuang, H., 2020b. Facile preparation of biosurfactant-functionalized Ti<sub>2</sub>CTX  
884 MXene nanosheets with an enhanced adsorption performance for Pb(II) ions. *Journal of Molecular  
885 Liquids* 297, 111810.

886 Won, S.W., Kotte, P., Wei, W., Lim, A., Yun, Y.-S., 2014. Biosorbents for recovery of precious metals.  
887 *Bioresource technology* 160, 203-212.

888 Wu, Y., Nie, P., Wang, J., Dou, H., Zhang, X., 2017. Few-layer MXenes delaminated via high-energy  
889 mechanical milling for enhanced sodium-ion batteries performance. *ACS applied materials & interfaces*  
890 9, 39610-39617.

891 Wu, Y., Pang, H., Liu, Y., Wang, X., Yu, S., Fu, D., Chen, J., Wang, X., 2019. Environmental remediation of  
892 heavy metal ions by novel-nanomaterials: a review. *Environmental pollution* 246, 608-620.

893 Xie, X., Chen, C., Zhang, N., Tang, Z.-R., Jiang, J., Xu, Y.-J., 2019. Microstructure and surface control of  
894 MXene films for water purification. *Nature Sustainability* 2, 856-862.

895 Xiu, L., Wang, Z., Yu, M., Wu, X., Qiu, J., 2018. Aggregation-resistant 3D MXene-based architecture as  
896 efficient bifunctional electrocatalyst for overall water splitting. *ACS nano* 12, 8017-8028.

897 Xu, X., Yang, T., Zhang, Q., Xia, W., Ding, Z., Eid, K., Abdullah, A.M., Hossain, M.S.A., Zhang, S., Tang, J.,  
898 2020. Ultrahigh capacitive deionization performance by 3D interconnected MOF-derived nitrogen-doped  
899 carbon tubes. *Chemical Engineering Journal* 390, 124493.

900 Yang, G., Hu, X., Liang, J., Huang, Q., Dou, J., Tian, J., Deng, F., Liu, M., Zhang, X., Wei, Y., 2021. Surface  
901 functionalization of MXene with chitosan through in-situ formation of polyimidazoles and its adsorption  
902 properties. *Journal of Hazardous Materials*, 126220.

903 Yang, H.-M., Hwang, J.R., Lee, D.Y., Kim, K.B., Park, C.W., Kim, H.R., Lee, K.-W., 2018. Eco-friendly one-  
904 pot synthesis of Prussian blue-embedded magnetic hydrogel beads for the removal of cesium from  
905 water. *Scientific reports* 8, 1-10.

906 Yang, X., Li, J., Liu, J., Tian, Y., Li, B., Cao, K., Liu, S., Hou, M., Li, S., Ma, L., 2014. Simple small molecule  
907 carbon source strategy for synthesis of functional hydrothermal carbon: preparation of highly efficient  
908 uranium selective solid phase extractant. *Journal of Materials Chemistry A* 2, 1550-1559.

909 Yang, X., Liu, Y., Hu, S., Yu, F., He, Z., Zeng, G., Feng, Z., Sengupta, A., 2020. Construction of Fe<sub>3</sub>O<sub>4</sub>@  
910 MXene composite nanofiltration membrane for heavy metal ions removal from wastewater. *Polymers  
911 for Advanced Technologies*.

912 Yang, X., Wan, Y., Zheng, Y., He, F., Yu, Z., Huang, J., Wang, H., Ok, Y.S., Jiang, Y., Gao, B., 2019. Surface  
913 functional groups of carbon-based adsorbents and their roles in the removal of heavy metals from  
914 aqueous solutions: a critical review. *Chemical Engineering Journal* 366, 608-621.

915 Ying, Y., Liu, Y., Wang, X., Mao, Y., Cao, W., Hu, P., Peng, X., 2015. Two-dimensional titanium carbide for  
916 efficiently reductive removal of highly toxic chromium (VI) from water. *ACS applied materials &*  
917 *interfaces* 7, 1795-1803.

918 Yusan, S.D., Akyil, S., 2008. Sorption of uranium (VI) from aqueous solutions by akaganeite. *Journal of*  
919 *hazardous materials* 160, 388-395.

920 Zhang, C.J., Pinilla, S., McEvoy, N., Cullen, C.P., Anasori, B., Long, E., Park, S.-H., Seral-Ascaso, A.s.,  
921 Shmeliov, A., Krishnan, D., 2017. Oxidation stability of colloidal two-dimensional titanium carbides  
922 (MXenes). *Chemistry of Materials* 29, 4848-4856.

923 Zhang, G., Wang, T., Xu, Z., Liu, M., Shen, C., Meng, Q., 2020. Synthesis of amino-functionalized Ti<sub>3</sub>C<sub>2</sub>T<sub>x</sub>  
924 MXene by alkalization-grafting modification for efficient lead adsorption. *Chemical Communications* 56,  
925 11283-11286.

926 Zhang, X., Liu, Y., 2020. Nanomaterials for radioactive wastewater decontamination. *Environmental*  
927 *Science: Nano* 7, 1008-1040.

928 Zhang, Y.-J., Lan, J.-H., Wang, L., Wu, Q.-Y., Wang, C.-Z., Bo, T., Chai, Z.-F., Shi, W.-Q., 2016. Adsorption of  
929 uranyl species on hydroxylated titanium carbide nanosheet: A first-principles study. *Journal of*  
930 *hazardous materials* 308, 402-410.

931 Zhang, Y., Wang, L., Zhang, N., Zhou, Z., 2018. Adsorptive environmental applications of MXene  
932 nanomaterials: a review. *RSC advances* 8, 19895-19905.

933 Zhu, H.-Y., Jiang, R., Xiao, L., 2010. Adsorption of an anionic azo dye by chitosan/kaolin/ $\gamma$ -Fe<sub>2</sub>O<sub>3</sub>  
934 composites. *Applied Clay Science* 48, 522-526.

935 Zhu, M., Huang, Y., Deng, Q., Zhou, J., Pei, Z., Xue, Q., Huang, Y., Wang, Z., Li, H., Huang, Q., 2016. Highly  
936 flexible, freestanding supercapacitor electrode with enhanced performance obtained by hybridizing  
937 polypyrrole chains with MXene. *Advanced Energy Materials* 6, 1600969.

938 Zou, G., Guo, J., Peng, Q., Zhou, A., Zhang, Q., Liu, B., 2016. Synthesis of urchin-like rutile titania carbon  
939 nanocomposites by iron-facilitated phase transformation of MXene for environmental remediation.  
940 *Journal of Materials Chemistry A* 4, 489-499.

941

942

943